Universitat Politècnica de Catalunya

Programa de Doctorat:

Automàtica, Robòtica i Visió

Tesi Doctoral

Control Structures and Optimal Sensor/Actuator Allocation: Application in Active Noise Control

Miquel À. Cugueró i Escofet

Director: Ricardo S. Sánchez Peña

Desembre de 2009

Als meus pares, Carme i Miquel

ABSTRACT

This thesis presents novel and applied work in the area of control and sensor/actuator (S/A) allocation in Active Noise Control (ANC) systems. First, robust identification and control techniques to perform ANC have been applied. The identification phase is based on a control-oriented robust identification approach that considers both parametric and nonparametric descriptions of the system, and quantifies the uncertainty. The controller design compares the feedback (FB), feedforward (FF) and hybrid (FB/FF) control structures. The feedback control is synthesized and evaluated in the robust control framework, and it is designed using $\mathcal{H}_\infty$ optimal control as a mixed-sensitivity problem. The FF controller is an adaptive identifier, based on the robustly normalized σ-algorithm. Two approaches are developed to decide which control structure is more efficient on a 4-m duct example with broadband noise. In addition, the compromises between identification and control, the inherent limitations of feedback and implementation issues in ANC are explicitly pointed out. Relations between performance, controller order, parametric/nonparametric models and digital signal processor (DSP) implementation are discussed. Theoretical and experimental results on the duct are compared. The gaps that still remain between theory and practice in this type of applications, are also outlined. Furthermore, this work considers the problem of quantifying the location of sensors and actuators in order to control a certain physical system. The measure to determine the best S/A location is based on a closed loop control-oriented criteria, which optimizes overall performance and practical implementation issues. In addition, it should be computed before the actual controller is designed, implemented and tested. The use of this measure minimizes the combinatorial controller testing over all possible S/A combinations. To this end, several measures have been defined which weight the potential closed-loop performance, robustness, plant condition number (input/output (I/O) relative gains) and implementation issues, such as the controller order. These may be computed with standard software, either for Single Input Single Output (SISO) models or Multiple Input Multiple Output (MIMO) models, and may be applied to many engineering problems: mechanics, acoustics, aerospace, etc. Here, these results are also illustrated with the prior ANC

example and validated against experimental data. The outcome of applying these measures is the selection of the S/A location which achieves the best closed loop noise attenuation with the lowest possible controller order.

Keywords: Active noise control, sensor/actuator allocation, $\mathcal{H}_\infty$ control, mixed sensitivity, hybrid (Feedforward/Feedback) controller.

Resum

Aquesta tesi presenta treball original i aplicat en l'àrea del control i la col·locació de sensors/actuadors (S/A) en sistemes de Control Actiu de Soroll (ANC). Primer, s'han aplicat tècniques de control i identificació robustes per a aconseguir ANC. La fase d'identificació està basada en una proposta d'identificació robusta orientada al control, considerant descripcions del sistema tant paramètriques com no-paramètriques, així com quantificant la incertesa. El disseny del controlador compara les estructures de control *feedback* (FB), *feedforward* (FF) i híbrida (FB/FF). El controlador *feedback* és sintetitzat i avaluat en el marc del control robust, i s'ha dissenyat utilitzant control òptim $\mathcal{H}_\infty$ plantejat com un problema de sensibilitats mixtes. El controlador FF és un identificador adaptatiu, basat en l'algorisme σ robustament normalitzat. S'han desenvolupat dues propostes per a decidir quina de les estructures de control és més eficient, aplicades a un conducte de 4 metres amb soroll de banda ampla. A més a més, s'han mostrat de manera explícita els compromisos entre identificació i control, les limitacions inherents a un llaç de control *feedback*, així com qüestions relatives a la implementació de sistemes ANC. També s'han tractat altres qüestions com la relació entre acompliment, ordre del controlador, models paramètrics/no-paramètrics i implementació en processadors digitals de senyal (DSP), així com s'han comparat resultats teòrics i experimentals en el conducte. Les llacunes que encara resten entre teoria i pràctica en aquest tipus d'aplicacions també s'han resumit. D'altra banda, en aquest treball també es tracta el problema de com quantificar la col·locació de sensors i actuadors, amb la finalitat de controlar un sistema físic determinat. La mesura per a determinar la millor localització de S/A es basa en un criteri de llaç tancat orientat al control, el qual optimitza tant acompliment com qüestions pràctiques d'implementació. Aquesta mesura hauria de calcular-se abans del disseny, implementació i prova del controlador. La utilització d'aquesta mesura minimitza la prova combinatòria de controladors en totes les possibles combinacions de S/A. Per a aconseguir-ho, s'han definit diferents mesures que pesen l'acompliment potencial en llaç tancat, la robustesa, el número de condició de la planta (guanys relatius entrada/sortida (I/O)) així com altres qüestions d'implementació, com l'ordre

del controlador. Aquestes poden calcular-se utilitzant *software* estàndard, tant per a models d'una-entrada-una-sortida (SISO) com per a models de múltiples-entrades-múltiples-sortides (MIMO) i poden aplicar-se a múltiples problemes d'enginyeria, ja siguin mecànics, acústics, aeroespacials, etc. En aquest treball, aquests resultats també s'han il·lustrat amb l'aplicació ANC presentada i validat amb dades experimentals. Com a resultat d'aplicar aquestes mesures, s'obté la localització de S/A que aconsegueix la millor atenuació del soroll en llaç tancat amb el menor ordre possible del controlador.

Paraules clau: Control actiu de soroll, distribució de sensors/actuadors, control $\mathcal{H}_\infty$, sensibilitats mixtes, controlador híbrid (Feedforward/Feedback).

Resumen

Esta tesis presenta trabajo original y aplicado en el área del control y la colocación de sensores/actuadores (S/A) en sistemas de Control Activo de Ruido (ANC). Primero, se han aplicado técnicas de control e identificación robustas para conseguir ANC. La fase de identificación está basada en una propuesta de identificación robusta orientada al control, considerando descripciones del sistema tanto paramétricas como no-paramétricas, así como cuantificando la incertidumbre. El diseño del controlador compara las estructuras de control *feedback* (FB), *feedforward* (FF) e híbrida (FB/FF). El controlador *feedback* es sintetizado y evaluado en el marco del control robusto, y se ha diseñado utilizando control óptimo $\mathcal{H}_\infty$ planteado como un problema de sensibilidades mixtas. El controlador FF es un identificador adaptativo, basado en el algoritmo σ robustamente normalizado. Se han desarrollado dos propuestas para decidir cual de las estructuras de control es más eficiente, aplicadas a un conducto de 4 metros con ruido de banda ancha. Además, se han mostrado de manera explícita los compromisos entre identificación y control, las limitaciones inherentes a un lazo *feedback*, así como cuestiones relativas a la implementación de sistemas ANC. También se han tratado otras cuestiones como la relación entre desempeño, orden del controlador, modelos paramétricos/no-paramétricos e implementación en procesadores digitales de señal (DSP), así como se han comparado resultados teóricos y experimentales en el conducto. Las lagunas que aún quedan entre teoría y práctica en este tipo de aplicaciones también se han resumido. Por otra parte, en este trabajo se trata también el problema de como cuantificar la colocación de sensores y actuadores, con la finalidad de controlar un sistema físico determinado. La medida para determinar la mejor localización de S/A se basa en un criterio de lazo cerrado orientado al control, el cual optimiza tanto desempeño como cuestiones prácticas de implementación. Esta medida debería calcularse antes del diseño, implementación y prueba del controlador. La utilización de esta medida minimiza la prueba combinatoria de controladores en todas las posibles combinaciones de S/A. Para conseguirlo, se han definido distintas medidas que pesan el desempeño potencial en lazo cerrado, la robustez, el número de condición de la planta (ganancias relativas entrada/salida (I/O)) y otras cuestiones de implementación, como el

orden del controlador. Éstas pueden calcularse utilizando *software* estándar, tanto para modelos de una-entrada-una-salida (SISO) como para modelos de múltiples-entradas-múltiples-salidas (MIMO) y pueden aplicarse a múltiples problemas ingenieriles, ya sean mecánicos, acústicos, aeroespaciales, etc. En este trabajo, estos resultados también son ilustrados con la aplicación ANC presentada y validados con datos experimentales. Como resultado de aplicar estas medidas, se obtiene la localización de S/A que consigue la mejor atenuación de ruido en lazo cerrado con el menor orden posible del controlador.

Palabras clave: Control activo de ruido, distribución de sensores/actuadores, control $\mathcal{H}_\infty$, sensibilidades mixtas, controlador híbrido (Feedforward/Feedback).

ACKNOWLEDGEMENT

The completion of an amusing research stage is attained with this work, and I would strongly like to thank all the people who contributed to reach it in one way or another.

I am especially in debt to my advisor Ricardo S. Sánchez Peña, for his infinite patience, guidance and help throughout this day-to-day work, managing well to go beyond the figure of advisor and always providing robustness to the uncertain moments.

I am also thankful to Professors Vicenç Puig, Joseba Quevedo and the entire SAC research group, to always give the assistance needed to go forward on my research. I am also indebted to Professor Jordi Romeu and all the people from the LEAM laboratory, providing a friendly space to work, and also all the facilities, useful comments and help always I needed.

Reviews, interesting comments and endless support received from Dr. Fernando Bianchi have been also uplifting in many fields involved in this work and gave priceless help which is also far worthy to be acknowledged. I am also grateful to Dr. Bernardo Morcego, for his aid and contribution since the early steps of my research subject.

Lots of inspiring moments also came from living together with all the people from the ESAII department in Terrassa, especially with my mates from Boeing office, Rosa, Carlos, Albert, Juli, Fernando, and nowadays Clàudia and David, with whom I have shared a lot in which I must say is like a second home to me.

I have no words to express the gratitude for the hand and understanding given by Isa, always close when most needed, and by my parents Mª del Carme and Miquel, my sister and my brother

Tali and Pep, my grandmothers Maria and Marina and my uncle Manel, for giving me a valuable model to follow in many ways, and for their precious aid and unconditional love given through my life.

<div align="right">

Miquel À. Cugueró i Escofet
Terrassa, December 2009

</div>

NOTATION

The notation used throughout the thesis is presented next:

F_ℓ	lower linear fractional transform
$\mathbf{p}$	filter parameters vector
z	performance variable
Δ	uncertainty
$\sigma(A)$	singular values of A
W_p	performance weight
W_δ	uncertainty weight
G_{pri}	primary circuit transfer function
G_{sec}	secondary circuit transfer function
G_o	nominal model
K	feedback controller
W	feedforward controller
G	augmented model
$\tilde{G}$	uncertain model
$\hat{G}$	estimate of G
$\mathcal{G}$	set of uncertain models
T_s	sampling time
S	sensitivity function
T	complementary sensitivity function
T_{zw}	closed loop transfer function
ω	frequency
Ω	frequency bandwidth
Ω_p	performance bandwidth
W_c	controllability grammian

W_o	observability grammian
κ	condition number
ρ_o	controller order measure
ρ_{p_d}	deterministic performance measure
$\rho_{\delta_{error}}$	error uncertainty measure
ρ_Ω	bandwidth uncertainty measure
ρ_m	uncertainty weight measure
e_{rel}	relative (multiplicative) model error
$\rho_{\gamma_{\min}}$	potential performance measure
ρ_κ	model condition number measure
ρ_{as}	general S/A measure
γ	robust performance measure
γ_z	RHP zeros robust performance lower limit
ς	RHP zero
λ	weighted attenuation
S_Δ	uncertain sensitivity function
$\mathcal{S}$	pair selection set
sup	supremum
$\underline{x}$	lower bound on x
$\overline{x}$	upper bound on x

ACRONYMS

ANC	Active Noise Control
DSP	Digital Signal Processor
FB	Feedback
FF	Feedforward
FFT	Fast Fourier Transform
FIR	Finite Impulse Response
IIR	Infinite Impulse Response
FXLMS	Filtered X Least Mean Squares
FULMS	Filtered U Least Mean Squares
HSV	Hankel Singular Values
I/O	Input/Output
LFT	Linear Fractional Transform
LMI	Linear Matrix Inequality
LTI	Linear Time Invariant
MIMO	Multiple Input Multiple Output
NP	Nominal Performance
RHP	Right Half Plane
RP	Robust Performance
RS	Robust Stability
SISO	Single Input Single Output
SOS	Second Order Sections
SS	State Space
S/A	Sensor/Actuator
TF	Transfer Function
ZP	Zero-Pole

CONTENTS

LIST OF TABLES

LIST OF FIGURES

CHAPTER 1

INTRODUCTION

1.1 Motivation

Active noise control has been a very active research area for many years, since the seminal ideas of [Lue34]. Today, the underlying principles are well established ([NE92, KM95]), but there are still many practical issues to be solved. The appearance of signal processors, *e.g.* DSP, has allowed ANC to become a feasible noise-suppression technology that has progressed from laboratory research to industrial implementation. A wide variety of applications that include aircraft engines, automobile interiors, heating, ventilation and air conditioning (HVAC) systems, as well as household appliances, have been produced. In general, ANC has been proven as a viable method for noise suppression in low-frequency ranges, where traditional passive noise control devices become massive, bulky, or less effective.

The ANC applications must deal with uncertain plants with time delays and/or zeros in the right half plane (RHP), lightly damped and fast dynamics, which need low order controllers for real time implementation. Uncertainty makes robust control approximations recommended in order to achieve stable behaviors, as highlighted by Hansen [Han04]. Also as recognized in [RGL02], robust identification techniques should be used to obtain a set of models which include uncertainty in case robust control techniques are used for controller design. Furthermore, duct physical modeling can be used for simulations purposes, but in the end an experimental identification procedure is needed when control is the final objective, as concluded in [HAV$^+$96].

So far, in ANC using robust techniques, models are obtained using classical parameter estimation, ARX [HAV$^+$96, BL97, BL98, CA00] or subspace techniques [OWPB00, KF03],

with no systematic way to produce a deterministic worst case uncertainty bound, see *e.g.* [BL98, KF03]. To the knowledge of the author, control oriented and/or robust identification methods as introduced in [HJN91] (see tutorials in [MPG95, CG00] and Chap. 10 of [SS98]) have not been systematically applied to identify and design robust controllers for ANC systems.

Design procedures which take into account the order of the final controller to implement, without forgetting other important issues like performance and robustness, should be also considered in the design stage. The selection of inputs and outputs affects the plant model identified and thus the performance and complexity of the resulting control system. In order to avoid combinatorial selection procedures, some *a priori* quantitative indexes considering these items would be useful to complete the designer experience and skill.

1.2   Thesis Objectives

This thesis will be focused on facing some of the current drawbacks on ANC systems stated in Section 1.1, using robust control strategies. Therefore, the main objectives of this work are presented next:

1. A practical application of robust (control oriented) identification to an ANC system (which accommodates the plant and uncertainty representation to the robust controller design framework) followed by a robust FB controller design for the same application. The implementation of the controller obtained is also presented in a real ANC example.

2. To explicitly point out the compromises and practical issues which arise in the robust identification and controller design stages for an ANC system. This will be helpful in some phases dealing with this application, like the controller design, the S/A allocation choice and/or the final real-time implementation of the controller in the actual ANC system.

3. To implement a robust FF control structure on an ANC (uncertain) system, in order to fulfill the stability demands of this kind of applications. This will be also implemented in an hybrid (FF/FB) fashion in order to compare the results obtained with these structures and the robust FB controller already implemented.

4. Last but not least, to create a methodology of optimal S/A allocation in order to consider issues such as controller order, performance and robustness before the controller design

and implementation. This measure should be general (*i.e.* usable in other applications) and give useful criteria to decide the best S/A distribution within a certain given set.

1.3 Outline of the Thesis

This dissertation is organized in several chapters, which can be briefly summarized as follows:

Chapter 2: Background and State of the Art

A state-of-the-art on control structures used in ANC applications is performed in this chapter. These include: *feedback*, *feedforward* and *hybrid* designs. Literature review related to S/A allocation is also presented.

Chapter 3: Experimental Setup

The application used to test the methodology presented in this work, *i.e.*, a laboratory duct prepared to implement ANC structures, is depicted in greater detail in this chapter.

Chapter 4: Feedforward Control Structures

Extensive research has been performed in the area of adaptive identification, as a means of producing *feedforward* controllers. Simple contributions to this area have been presented in [CSM$^+$05] and in [MC01], where a comparison between *feedforward* algorithms and a DSP implementation discussion of these structures are performed, respectively. Furthermore, robust adaptive *feedforward* algorithms (*e.g.* [IS96]) consider the convergence problem, *i.e.* stability, but are not generally applied to ANC systems (*e.g.* [DH09], [WL05]). Some results achieved with this kind of *feedforward* robustly-adaptive algorithms, also presenting performance of the loop in a real ANC system, are illustrated by the author in [CMS07] and condensed in Chapter 6 of this work. In Chapter 4, the preliminaries to implement conveniently this robustly-adaptive *feedforward* algorithms and control structures in an ANC application are stated.

Related Publications

[CSM⁺05]   M.À. CUGUERÓ, R.S. SÁNCHEZ PEÑA, A. MASIP, B. MORCEGO, J. QUEVEDO,
V. PUIG, T. PÀMIES AND J. ROMEU. Comparación de Algoritmos FeedForward
Adaptativos para el Control Activo de Ruido. In *Proceedings of Tecniacústica 2005*,
Terrassa, Barcelona, 2005.

[MC01]   B. MORCEGO AND M.À. CUGUERÓ. Comparación de implementaciones en C y
Matlab de filtros adaptativos para DSP. In *Proceedings of XXII Jornadas de Au-
tomática*, Bellaterra, Barcelona. 2001.

Chapter 5: Feedback Control Structures

In this chapter, robust *feedback* design methodologies, such as robust (control oriented) identi-
fication and/or robust controller design, are introduced and applied to an ANC real system (see
[SCM⁺05, PnCM⁺08]). The robust identification method presented produces a multiplicative
global uncertain set to describe the physical plant, which exactly fits the robust controller design
framework. These methodologies are applied to an ANC real system and the results obtained
are presented.

Related Publications

[PnCM⁺08]   R.S. SÁNCHEZ PEÑA, M.A. CUGUERÓ, A. MASIP, J. QUEVEDO AND V. PUIG.
Identification and Feedback Design: an Active Noise Control Case Study. *Control
Engineering Practice*, 16(11):1265-1274, NOV 2008.

[SCM⁺05]   R.S. SÁNCHEZ PEÑA, M.A. CUGUERÓ, A. MASIP, J. QUEVEDO AND V. PUIG.
Acoustic Noise Suppression: Compromises in Identification and Control. In *Pro-
ceedings of 2nd. International Conference on Informatics in Control, Automation
and Robotics*, Barcelona, 2005.

Chapter 6: Hybrid (Feedforward/Feedback) Structures

Hybrid structures, mixing both FB and FF designs, and results achieved with them, are also an important part of this work. Its advantages and disadvantages, as well as the practical issues which can be found when implementing them in an hybrid fashion and/or separately are considered in great detail. *Feedback* structures applied in ANC usually produce less performance (compared with *feedforward* ones) because of their intrinsical limitations, which have been extensively studied since the 1980s (see [FHMT03]). This is at the expense of a greater robustness both for stability and performance. Some results comparing all these structures applied to an ANC real system are also presented in this chapter (see [CMS07]).

Related Publications

[CMS07]   M.A. CUGUERÓ, B. MORCEGO AND R.S. SÁNCHEZ PEÑA. Identification and Control. The Gap between Theory and Practice, *chapter 8. Identification and Control Structure Design in Active (Acoustic) Noise Control*, pp. 203-44. Springer-Verlag. 2007.

Chapter 7: Sensor/Actuator Allocation

The final contribution of this thesis is to face the S/A allocation as part of the identification and control scheme. S/A allocation is an important issue in ANC applications, and it seems convenient, in order to reach high performances, to have a criteria to optimize it as part of the whole problem. The first proposal in this research line is a new criteria to define the optimality of S/A allocation, tested against a validated simulation case [SPCiE08]. Next, this criteria has been improved and tested in a real application (see [CSPn09]) using the acoustic duct in LEAM laboratory (UPC, Terrassa) where some of the prior works have been already developed (see [Rom99, SCM$^+$05, PnCM$^+$08, CMS07]).

Related Publications

[CSPn09]   M.A. CUGUERÓ AND R.S. SÁNCHEZ PEÑA. Control-Oriented Sensor/Actuator
            Location measures. *Control Engineering Practice*, (submitted), 2009.

[SPCiE08] R.S. SÁNCHEZ PEÑA AND M.A. CUGUERÓ. Control-Oriented Sensor/Actuator
            Location Measures for Active Noise Control. In *Proceedings of IFAC World
            Congress*, Seoul, South Korea, pages 8719-8724, 2008.

1.3.1   Compilation of Related Publications

The publications related to this work are compiled all together next:

Book chapters:

[CMS07]   M.A. CUGUERÓ, B. MORCEGO AND R.S. SÁNCHEZ PEÑA. Identification and
            Control. The Gap between Theory and Practice, *chapter 8. Identification and Con-
            trol Structure Design in Active (Acoustic) Noise Control*, pp. 203-44. Springer-
            Verlag. 2007.

Journal papers:

[CSPn09]   M.A. CUGUERÓ AND R.S. SÁNCHEZ PEÑA. Control-Oriented Sensor/Actuator
            Location measures. *Control Engineering Practice*, (submitted), 2009.

[PnCM$^+$08] R.S. SÁNCHEZ PEÑA, M.A. CUGUERÓ, A. MASIP, J. QUEVEDO AND V. PUIG.
            Identification and Feedback Design: an Active Noise Control Case Study. *Control
            Engineering Practice*, 16(11):1265-1274, NOV 2008.

Conference papers:

[SPCiE08] R.S. SÁNCHEZ PEÑA AND M.A. CUGUERÓ. Control-Oriented Sensor/Actuator
            Location Measures for Active Noise Control. In *Proceedings of IFAC World
            Congress*, Seoul, South Korea, pages 8719-8724, 2008.

[SCM+05] R.S. SÁNCHEZ PEÑA, M.A. CUGUERÓ, A. MASIP, J. QUEVEDO AND V. PUIG. Acoustic Noise Suppression: Compromises in Identification and Control. In *Proceedings of 2nd. International Conference on Informatics in Control, Automation and Robotics*, Barcelona, 2005.

[CSM+05] M.À. CUGUERÓ, R.S. SÁNCHEZ PEÑA, A. MASIP, B. MORCEGO, J. QUEVEDO, V. PUIG, T. PÀMIES AND J. ROMEU. Comparación de Algoritmos FeedForward Adaptativos para el Control Activo de Ruido. In *Proceedings of Tecniacústica 2005*, Terrassa, Barcelona, 2005.

[MC01] B. MORCEGO AND M.À. CUGUERÓ. Comparación de implementaciones en C y Matlab de filtros adaptativos para DSP. In *Proceedings of XXII Jornadas de Automática*, Bellaterra, Barcelona. 2001.

CHAPTER 2

BACKGROUND AND STATE OF THE ART

2.1 Introduction

Control system design involves six well differentiated steps, as indicated in ([vdWdJ01]). First, control goals have to be considered, as the choice of variables like the exogenous variable w or the performance variable z. The second choice is the plant model G selection. In the third step, the control structure is selected, and in the fourth the controller K is designed according to the previous selections. After, in the fifth step, the closed-loop obtained is evaluated to see if the control goals are reached. Last but not least, in the sixth step the controller and the hardware are implemented in the real plant to see if the requirements are reached there. This is an iterative procedure, due to that are some adjustments that must be performed to get the desired behavior at the end.

Focusing on third and fourth steps, the most widely used approach for ANC in practical applications is based on the use of adaptive FF algorithms, because they can automatically modify the model characteristics and do not need a previous identification stage (see details in Section 2.2). The FF–ANC efficiency usually depends on how accurately the online model adjusts the primary path transfer function, and could suffer from possible instability. As noticed in [KM95, BL97], this does not preclude the use of feedback or hybrid (feedback/feedforward) control structures. The feedback control structure of an ANC system was first introduced in [OM53]. In this scheme, the system only requires the downstream error sensor. Unfortunately, this configuration provides poor broadband noise attenuation over a limited frequency range due to the spillover effect. A complete study of the limitations of feedback in ANC has been presented in [HB98] and corrected and generalized in [FHMT03], mainly based on the classical

9

limitations of feedback loops ([FL85, SBG97]). However, if a nonacoustical reference signal is not available and/or the order of the system is small, feedback control should be a feasible approach ([RE99]). Furthermore, many applications can only deal with noise through a feedback control loop, *e.g.* headsets, windows ([RE99, KPM03]). Finally, hybrid control combines both FF and FB, which could potentially ([WL05]) add up the benefits of both approaches. Nevertheless, it is not always clear if this is so in practice. In this work, two different approaches are developed that compare hybrid *versus* FF and FB controllers, as well as a systematic way of anticipating its possible benefits.

Plant uncertainty is one of the major contributing factors that affects performance and stability, in particular in ANC systems ([BL98]). It may be caused by modeling, computational, and/or measurement errors, or even perturbations in physical conditions. These factors lead to deviations of the plant from the nominal model, which should be considered at the control synthesis stage so that the closed loop is robust. Most robust control design methods dealing with uncertain models use a worst-case deterministic criterion to describe uncertainty, *e.g.* IMC or $\mathcal{H}_\infty$ optimal control ([BL97, BL98, THC02, KPM03]). Physical modeling can be used for simulation purposes, but in the end an experimental identification procedure is applied when control is the final objective, as concluded in [HAV$^+$96]. Usually, models are obtained using classical parameter-estimation ([BL97]) and there is no systematic way to produce a deterministic uncertainty bound ([KPM03]). The area of control-oriented and/or robust identification ([CG00], Chapter 10 of [SS98]) is instrumental in the design of robust controllers for ANC applications. Further explanations of the methodology used in the identification of the ANC problem presented in this work are given in Section 5.2 .

Here, adaptive FF, $\mathcal{H}_\infty$ FB and hybrid controller structures are systematically analyzed based upon the identification and controller robustness and performance experimental results, as suggested in [BL97]. Quantitative results at the identification stage using two different approaches, indicate if an hybrid controller adds extra benefits to a more standard FF adaptive one.

2.2   Adaptive Identification

The term adaptive is usually related in the literature to online control techniques. The term identification, conversely, is related to offline parameter-estimation techniques. Adaptive Identification deals with online parameter-estimation techniques and makes use of results from both areas.

Adaptive identification algorithms have been used in the area of adaptive control systems for a very long time, both for feedback (FB) and/or feedforward (FF) approaches [GS84, Tao03]. Usually for simplicity and computational speed in real time applications, parametric linear schemes have been implemented: RLS, NLMS, FXLMS, FULMS, as in the case of Active noise control [KM95], for example.

The application studied in this work, ANC, does not follow the typical closed-loop control scheme. Figure 2.1 shows a block diagram of the system and its control blocks. It can be observed that the error signal is located at the output of the system, while the input signal cannot be altered because it is the noise source. The controller's main function is to identify the dynamics of the sound-propagation system and to generate the opposite signal, thus producing as much silence as possible. Figure 2.1 also shows that the controller is laid out in a feedforward fashion. The sound-propagation system, a duct in the present case, suffers from slow dynamics variations due to *e.g.* temperature and humidity changes. It also collects sudden external noise perturbations and pressure variations at its end. In view of this, the main task of an active noise controller is to adaptively identify the sound-propagation system.

An important difficulty with this kind of control structure is to maintain and assure stability. One of the main concerns in this work is to deal with stability explicitly. Stability is an important issue for different reasons. On the one hand, there are physical reasons: the output loudspeaker is a nonminimum phase system and, as will be seen later in Section 4.1, its transfer function is susceptible to be inverted in some situations; in addition, one of the main characteristics of this kind of systems is their intrinsic delays, which also need to be accounted for, bringing up stability considerations. On the other hand, up to the knowledge of the author, the algorithms and filter structures used for noise cancelation do not consider robust stability criteria in general. [DFSVB01] faces the problem of designing robust feedforward control systems for ANC applications with single tone disturbances in a simulated fashion, based on a LMS-like solution. Other alternatives to the state-of-the-art algorithms that are intrinsically stable can be seen
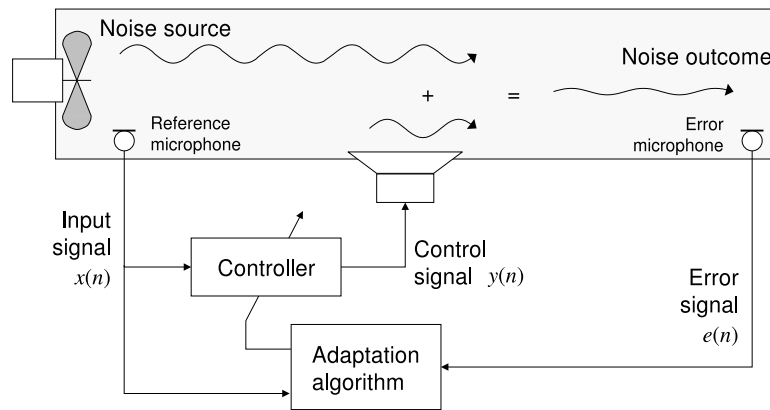
Figure 2.1: Simplified conceptual adaptive FF system block diagram

in [GSPnM07] and are also presented in a real application case in this work (see sections 4.2.1 and 4.2.2).

2.3   Sensor/Actuator Allocation

Input/Output selection, which is an important part of this work, is involved in the third step of the methodology explained in [vdWdJ01], that is control structure selection. This determines the number, place, and the type of actuators and sensors. The choice of inputs and outputs affects the performance, complexity, and costs of the control system. The selection problem is combinatorial in nature and hence, quantitative measures are needed to complement the design engineer's intuition, insight and experience.

Many works have been generated in this area, particularly for flexible structure testing ([LAKB01], chapter 7 of [Gaw04] and references therein, or more recent ones like [SFN08], [BK08], [RN08], [Mor08], [SBS$^+$09] and references therein) and process control ([SP96] and references therein). The definition of the S/A location problem is somewhat different for flexible structure testing, where the $\mathcal{H}_2, \mathcal{H}_\infty$ or Hankel norm needs to be maximized with the least amount of sensors and actuators [Gaw04], than for control-oriented applications. An excellent overview of the whole area and many other different applications can be found in [vdWdJ01]. Some recent contributions in the area can be found in [SFN08], where a criteria based on the controllability Grammian is used to find the optimal placement of a piezoelectric actuator to

suppress vibrations in a Finite Element model of a cantilevered beam. This is similar to the results in [SBS+09], where a criteria to place piezoelectric sensor and actuators is applied in order to minimize the magnitude of the natural frequencies on the same element. Also in [BK08], a study about collocation/non-collocation of actuators and sensors and model truncation has been performed in order to see how stability is affected, using the S/A placement criteria from [Gaw97] and [Gaw99]. In [Mor08], optimal placement of actuators is performed to improve performance of an LQR by means of solving an algebraic Ricatti equation.

For Active Noise Control (ANC) in particular, there are several works to be cited. In [KTMX95, RF95] actuator placement is studied for active noise control and [DF99] focuses on the efficiency of manipulation. More recent works as [PP06] or [PP08] have been extended to uncertain model sets with dynamic uncertainty. In [LAKB01] a magnitude to measure the optimal S/A locations based on the controllability (W_c) and observability (W_o) grammians is computed. In [PP06] another measure is added to consider the effect of model uncertainty. Nevertheless, these grammians depend on the particular state-space realization, therefore any measure derived from it could be misleading. Furthermore, the sensor and actuator location problems are treated separately, by means of two different measures, one depending on W_c, the other on W_o. This could produce situations where a good location of the sensor (good observation properties) could interact with a bad location of the actuator (poor control action) and viceversa.

From a very general point of view, in [vdWdJ01] different S/A allocation methods have been compared based on eight characteristics: well-founded, efficient, effective, applicability, rigorous, quantitative, controller independent and direct. There, although the general control configuration in Figure 2.2 was used, the performance limitations for that structure where not yet available [FHMT03]. This general setting and the previous references indicate that robust performance oriented measures have not been computed previously under a controller independent constraint. Furthermore, controller complexity (basically controller order) should be integrated with other relevant issues, *e.g.* robustness and performance. Finally, several indexes seem to be necessary and hence a combination of these S/A measures should be applied for practical purposes. An approach of these indexes measuring controller complexity, robustness and performance under a controller independent constraint is developed and applied in Chapter 7 of the present work.
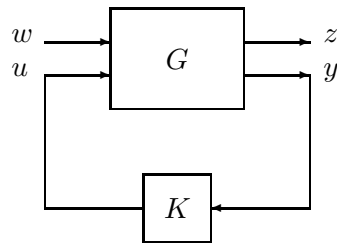
Figure 2.2: Control design structure $T_{zw} = F_\ell\left(G, K\right)$.

CHAPTER 3

EXPERIMENTAL SETUP

3.1 Description

The application used along this work is illustrated in Figure 3.1. It is a square, 4.85 meter long tube connected to a semianechoic[1] room (Figure 3.2), the other end connected to a noise generator, either a speaker or an industrial fan. This (primary) speaker generates noise in a certain controlled frequency bandwidth by means of a signal generator, and may physically simulate different noise sources. The advantage is that this noise source setup has a linear time invariant (LTI) behavior and precise experiments on the duct can be carried out. The industrial fan, however, is a real noise source with time-varying and nonlinear characteristics.

There is also an error microphone near the control actuator (secondary speaker) and one near the noise source, known as the reference microphone. The microphones are omnidirectional BEHRINGER ECM8000 with linear frequency response within a bandwidth of 15 Hz to 20 kHz and -60 dB acoustic sensitivity.

The speakers are BEYMA model 5 MP60/N of 5", 50W, with a bandwidth of 50Hz to 12kHz.

The secondary acoustic circuit is the one related to the feedback-control section, with the control speaker as the input and the error microphone as the output (Figure 3.4). The path covered by the perturbation signal which enters the error microphone coming from the acoustic path, with its origin in the noise source, is usually defined as the primary circuit.

---

[1]These rooms have a nonabsorbing floor, hence the sound measurement also depends on the floor reflection. This is not a problem in this application.

Control loops implemented run on a DSpace DSP-based (Texas Instruments TMS320C40 over a DS1003.05) floating-point processor board, as well as with a more recently acquired PowerPC-based on a IBM PowerPC 750GX. The sampling time for the identification experiments and control implementation is $T_s = 0.4$ms, which is good enough for the real-time computations needed in this kind of application. The complete signal-processing instrumentation is illustrated in Figure 3.3.

The off-line plant identification and FB controller synthesis have been programmed using standard Matlab, plus the additional functions in the Robust Control Toolbox ([BCPS05]) and other *ad-hoc* function packs as the Robust Identification Toolbox ([MPS04]). The main structure of the algorithm implemented can be found in Appendix A.

Furthermore, in order to final implement the control loops, the DSpace system comes with additional software. This includes a Matlab Toolbox allowing the interaction with the hardware using Simulink programming (which can pick up workspace data as usual) and also some C programming tools to use C code instead. In this work, both ways of programming have been used, depending on the specifications of each algorithm.

Figure 3.1: Tube and input noise source (fan)

The control scheme applies the classical method ([Lue34, OM53]) of generating a signal as close as possible to the real noise but with opposite phase. In this work, this will be performed in

Figure 3.2: Semianechoic room and tube output signal (arrow)
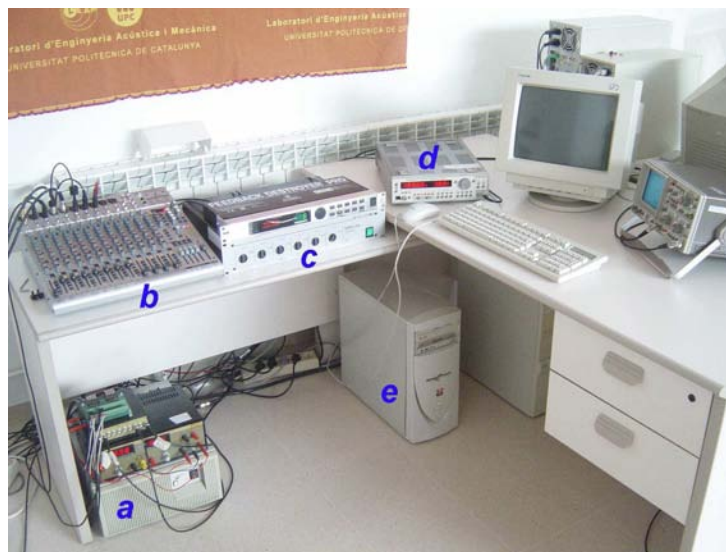
Figure 3.3: Signal-processing instrumentation composed by (a) DSpace system, (b) mixing console, (c) audio amplifier, (d) signal generator, (e) host PC, plus the oscilloscope

(a)

(b)
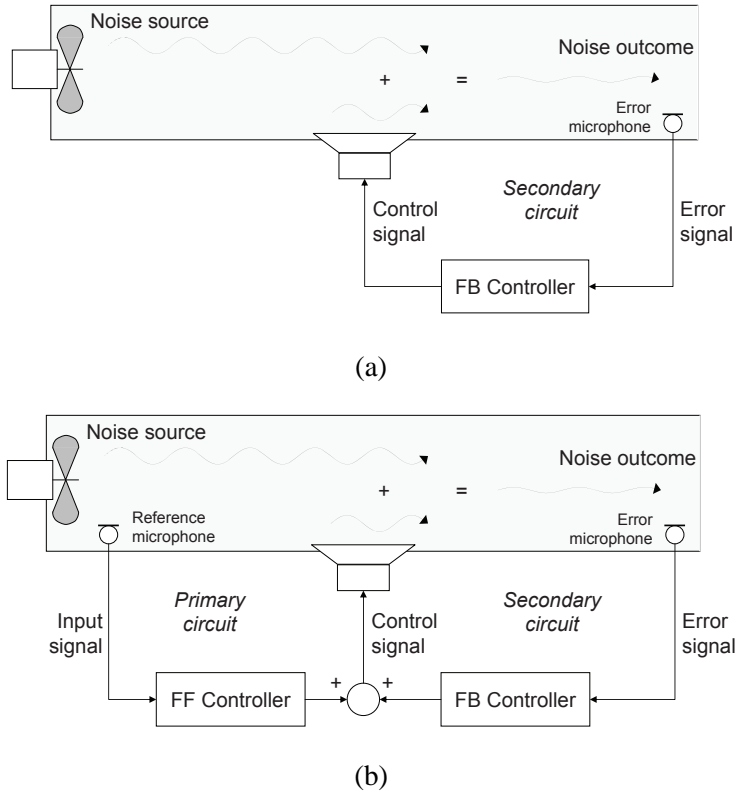
Figure 3.4: Conceptual view of acoustic noise suppression, (a) Feedback
scheme (b) Hybrid scheme

three ways: by fixed $\mathcal{H}_\infty$ *feedback* (FB) control, adaptive *feedforward* (FF), and also combined as an *hybrid* (FB/FF) controller, conceptually illustrated in Figures 2.1 and 3.4.

3.2   Physical Modeling

In this section, the main results on mathematical models for sound fields in rectangular tubes, such as the one proposed, are presented.

According to [HAV$^+$96] and [BL98], below the cutoff frequency, the sound field in the duct can be treated as unidimensional with spatial coordinate $x \in [0, 1]$. The control loudspeaker is located at $x = x_s$, while the feedback microphone is located at $x = x_m$. A state-space model

of the acoustic duct can be developed from three fundamental equations: the state equation, the continuity equation and the linearized inviscid force equation. Retaining r modes from such equations allows the duct state-space model to be derived with the structure in (3.1):

$$
\begin{aligned}
\dot{x}_d(t) &= A_d x_d(t) + B_d(t) u_s(t) \\
y_d(t) &= C_d x_d(t)
\end{aligned}
\tag{3.1}
$$

where:

$$
\begin{aligned}
x_d(t) &= \begin{bmatrix} q_1(t) & \dot{q}_1(t) & \cdots & q_r(t) & \dot{q}_r(t) \end{bmatrix}^T \\
A_d &= \text{block-diag}\left(\begin{bmatrix} 0 & 1 \\ -\omega_{n1}^2 & -2\xi_1\omega_{n1} \end{bmatrix}, \cdots, \begin{bmatrix} 0 & 1 \\ -\omega_{nr}^2 & -2\xi_1\omega_{nr} \end{bmatrix} \right) \\
B_d &= \begin{bmatrix} 0 & b_1 & \cdots & 0 & b_r \end{bmatrix}^T ; \quad C_d = \begin{bmatrix} V_1(x_m) & 0 & \cdots & V_r(x_m) & 0 \end{bmatrix}
\end{aligned}
$$

This model can be extended even further by including the transfer function from the speaker voltage input V_s to the speaker baffle acceleration $\dot{v}_s$ given by:

$$
\frac{s v_s(s)}{V_s(s)} = \frac{K_s s^2}{s^2 + 2\xi_s \omega_{ns} + \omega_{ns}^2}
\tag{3.2}
$$

that leads to a state-space vector of order $n = 2r + 2$.

However, according to [HAV$^+$96], the parameters of such a state-space model should be obtained by experimental identification. Therefore, a (control-oriented) identification technique has been performed in order to fit a nominal model plus a frequency-dependent model uncertainty bound to the (noisy) frequency response with a worst-case criteria (usually the fitting is in a least-squares sense, see [HAV$^+$96] and [BL98]). Furthermore, the previous mathematical model supports the fact that the nominal model should have parametric information based on second-order systems tuned to the modal frequencies of the duct. In this approach, further described in Section 5.1, this is performed *via* a finite set of Kautz orthonormal bases, which also serves to keep the model order as low as possible ([PSS99]).

CHAPTER 4

FEEDFORWARD CONTROL STRUCTURES

Feedforward adaptive control designs (see [KM95, WP97]) are commonly used in practical ANC applications, because they offer good performance and plant parameter adaptation, but in general they lack on robustness. This can be found in the introductory section of chapter 8 in [CMS07]. In this chapter, these structures applied to ANC and its robustness implications will be discussed.

4.1   Classical Feedforward Structures

Feedforward ANC systems are implemented using two different control structures, FXLMS and FULMS, standing for filtered X and filtered U least mean squared algorithms (see [KM95]). These control structures stem from different models or interpretations of the system, which will be explained in the following paragraphs.

The first *naive* model of the acoustic duct neglects the dynamics of the sensors and the actuator, and also neglects the propagation of the cancelation signal upstream and downstream of the duct. In this model, shown in Figure 4.1, the output signal $e = w - y = [G_{pri}(z) - W(z)]\,x$ becomes zero when $G_{pri}(z) = W(z)$. This means the controller $W(z)$ is exactly representing the dynamics of the duct, with a phase difference of 180 degrees.
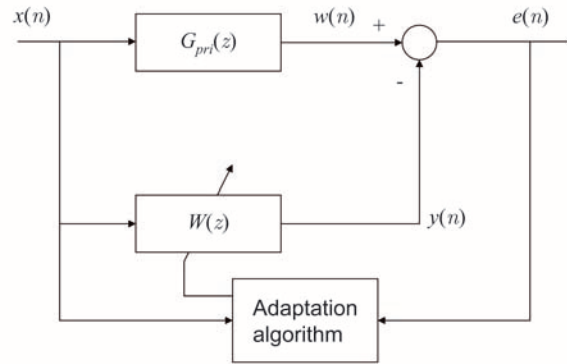
Figure 4.1: *Naive* model of the acoustic duct with controller

The most widely used cancelation algorithm is FXLMS, based on the model shown in Figure 4.2. This model includes the secondary path, which is the propagation dynamics that modifies signal $y(n)$ through the cancelation speaker and the downstream portion of the duct to the error microphone. Refining slightly the previous model of the system one can distinguish sev-
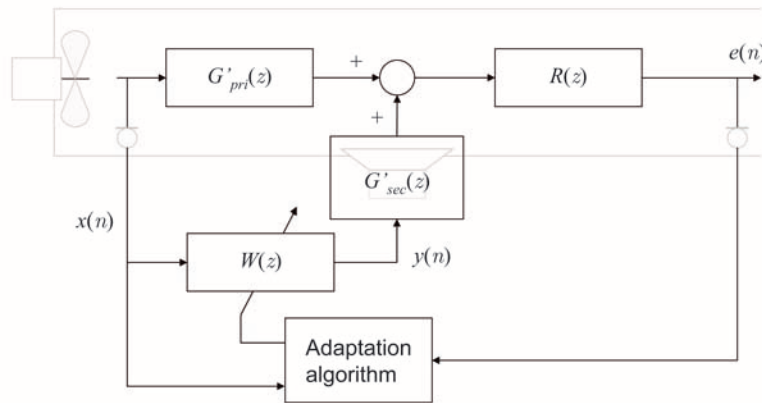
Figure 4.2: Block diagram of the duct system including the secondary path

eral elements that were ignored. On the one hand, signals $x(n)$ and $e(n)$ are captured with the reference and the error microphones, respectively. These signals are then amplified, filtered and digitalized. On the other hand, signal $y(n)$ is converted to analogical, amplified and delivered

by a loudspeaker. Then, once signal $y(n)$ is in the duct, it must travel some distance to reach the error microphone. All these elements are captured in the transfer functions shown in Figure 4.2, but considering that both signals $G'_{pri}(z)x$ and $G'_{sec}(z)y$ pass through the same piece of duct, modelled by $R(z)$, assuming linear dynamics and using

$$G_{pri}(z) = R(z)G'_{pri}(z)$$
$$G_{sec}(z) = R(z)G'_{sec}(z)$$

(4.1)

it is possible to represent the same model in a more convenient way, as shown in Figure 4.3.
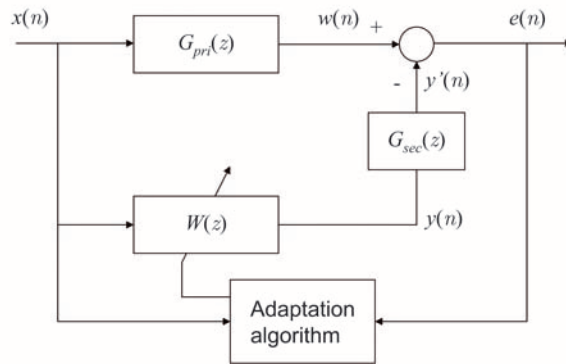
Figure 4.3: Simplified block diagram of the duct system including the
secondary path

Considering

$$E(z) = R(z)[G'_{pri}(z) - G'_{sec}(z)W(z)]X(z)$$

and using Equation (4.1), it is easy to see that when the error signal $e(n)$ goes to zero, that is when the filter $W(z)$ has converged, its transfer function is:

$$W(z) = \frac{G_{pri}(z)}{G_{sec}(z)}$$

(4.2)

Equation (4.1) reveals two important details of the cancelation filter $W(z)$. First, if the overall delay of the secondary path is larger than the delay of the primary path, the filter will not be realizable. This is the limiting causality constraint of FXLMS and FULMS control structures.

Second, if the secondary-path transfer function is nonminimum phase, then $W(z)$ becomes unstable. In fact this is what usually happens, due to loudspeaker's dynamics. Therefore, to compensate the undesirable effect of the secondary-path, some modifications need to be done.

There are some ways to perform this, as suggested in [Mor80], like post-filter $y(n)$ by $1/G_{sec}(z)$ or implement the FXLMS algorithm instead of the conventional LMS rule. The FXLMS algorithm is generally the most convenient approach, since an inverse of $G_{sec}(z)$ does not necessarily exist.

To understand the derivation of the FXLMS algorithm it is necessary to assume that the parameters in $W(z)$ are calculated with an LMS-like (or gradient descent) algorithm. In this case the error to minimize is given by Equation (4.3)

$$e \;=\; w - y' = w - G_{sec}(z)W(z)x \tag{4.3}$$

but considering slow filter parameter variations, or linear dynamics, the position of $W(z)$ and $G_{sec}(z)$ in Equation (4.3) can be swapped over. Gradient descent algorithms need to calculate the gradient of the error with respect to the parameters,

$$\nabla e = -G_{sec}(z)x \tag{4.4}$$

According to Equation (4.4), the parameter adaptation algorithm must be fed with a filtered version of signal $x(n)$. The filter should be the secondary-path transfer function, $G_{sec}(z)$, which is not available but can be estimated either online or offline. A more suitable expression of $\nabla e(n)$ would be

$$\nabla e = -\hat{G}_{sec}(z)x = -x'$$

where $\hat{G}_{sec}(z)$ is the estimate of $G_{sec}(z)$, which could be well computed either off-line, if time-invariant characteristic is assumed for $G_{sec}(z)$, or on-line, if potential real-time changes on its dynamics are assumed to be non-negligible. The previous transformations modify the control structure shown in Figure 4.3 leading to the one shown in Figure 4.9, where $W(z)$ is now fed with $x(n)$ and the adaptation algorithm is fed with $x'(n)$. Of course, there are many important practical and theoretical considerations related to the accuracy of $\hat{G}_{sec}(z)$, *e.g.* [SH94, BEN91, FBL93], but they will not be taken into account here for the sake of brevity.

The FXLMS control structure, although being one of the most widely used, considers an
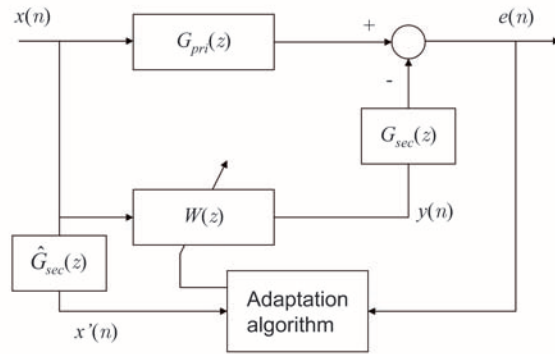
Figure 4.4: Standard control scheme of FXLMS

incomplete model of the system. The output signal $y(n)$ is fed into the acoustic duct through the secondary loudspeaker and is meant to counteract signal $G_{pri}(z)x$. When a signal is inserted into the duct, it travels both downstream and upstream. The effects of $y(n)$ upstream are ignored by the FXLMS algorithm, but they should be considered in order to avoid its non desirable effects, such as acoustic feedback on the reference microphone. There are some ways to face this problem, *e.g.* use non-acoustic sensing for the reference signal. The FULMS control structure, which will be presented next, is another possible solution to this problem.

The acoustic feedback, shown in Figure 4.5 as transfer function $F(z)$, is the effect of signal $y(n)$ on signal $x(n)$, as a result of having been captured by the reference microphone. The transfer function $F(z)$ models the digital-to-analog conversion of signal $y(n)$ and the upstream dynamics of the duct until the reference microphone is reached. Neglecting the effects of acoustic feedback is not as dangerous as neglecting secondary-path effects, but from Figure 4.5 it may be seen that the transfer function of the cancelation filter in Equation (4.5) could become unstable if the product $W(z)F(z)$ become larger than the unity at some frequency.

$$\frac{Y(z)}{X(z)} = H(z) = \frac{W(z)}{1 - W(z)F(z)} \tag{4.5}$$

The best way to counteract feedback effects is, as suggested previously, to minimize the acoustic feedback, for instance, using a non-acoustic transducer for the reference signal (like a piezoelectric sensor) instead of a microphone. Unfortunately, this is not always possible, hence it is useful to include an acoustic feedback cancelation filter in the control structure. This measure makes
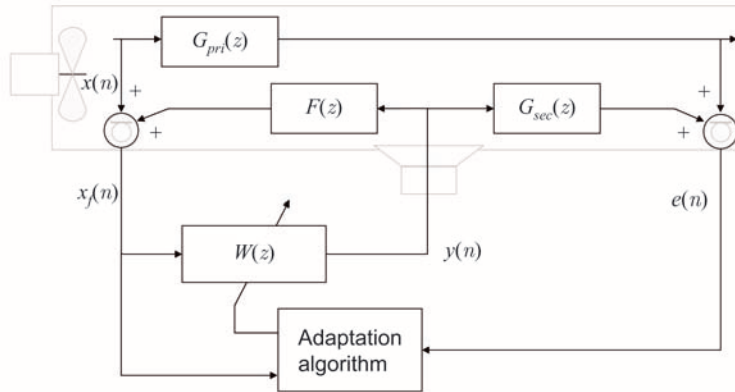
Figure 4.5: Model of the duct with the secondary path and the acoustic feedback

the overall control algorithm more complex, but it adds robustness and performance as compensation.

The FULMS control structure is shown in Figure 4.6. Its relation with FXLMS is very simple: the cancelation filter in FXLMS, an FIR filter, becomes an IIR filter un FULMS, *i.e.* a rational transfer function with poles.

From Figure 4.6, the transfer function presented in Equation (4.5) can be redefined as

$$\frac{Y(z)}{X(z)} = \frac{A(z)}{1 - B(z)}$$

which is the usual configuration of an IIR filter, where $A(z) = W(z)$ and $B(z) = D(z)\hat{F}(z)$.

The control structure shown in Figure 4.6 includes filters $A(z)$ and $B(z)$, as well as the estimation of the secondary-path transfer function, $\hat{G}_{sec}(z)$, needed to eliminate the instability effects of modeling its inverse. As it can be seen, using this control structure the acoustic feedback $F(z)$ is modeled in the feedback function $B(z)$.

The main drawback of IIR filters with LMS-like adaptation rules is that neither convergence nor stability of the solution is assured. In fact, many practical situations give evidences that IIR filter can become unstable quite easily, *e.g.* [And85].
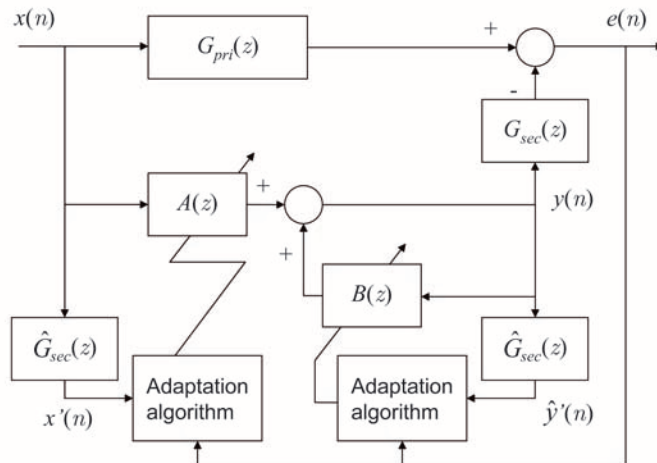
Figure 4.6: FULMS control structure

4.2 Robustness in Adaptive Identification

4.2.1 Relation between Robust Adaptive Identification and Classical Feedforward Structures

As stated earlier, this work is about active noise cancelation, but a fundamental concern is to ensure the stability of the solution.

Most active noise-control solutions (commercial or not) are based on gradient-descent algorithms. In fact, the most widely used algorithm is LMS, mainly for speed of execution, which allows a large number of parameters to be used in the cancelation filters. Many of those applications try to ensure the stability of their solutions by using proven control structures, such as FXLMS, or by carefully accomplishing physical laws that are known to maximize the effect of cancelation systems. However, there is little concern with the robustness of the algorithms employed.

Control researchers became very active in the late 1980s in the area of robust adaptive control (see [OT89]), showing, for example, that an adaptive scheme designed for a plant model without disturbances considerations could go unstable in the presence of small disturbances ([IS96]). They also developed a considerable number of robust adaptive laws and proved, in

each case, their robustness properties against different kinds of unstructured perturbations.

The adaptive algorithm used throughout this work in order to estimate the feedforward filter parameters is robust. The algorithm is the normalized LMS estimator with the σ-modification, which will be explained next (see [IS96] for a more detailed description).

The LMS algorithm, developed by Widrow [KD70], or the steepest-descent algorithm, presented in [KM95], are both examples of gradient-descent-based algorithms. The latter can be implemented using Equation (4.6)

$$\mathbf{p}(n+1) = \mathbf{p}(n) - \frac{\mu}{2}\nabla\xi(n) \tag{4.6}$$

where $\mathbf{p}$ is the parameter vector, $\nabla\xi(n)$ is the gradient of the error function with respect to $\mathbf{p}$ and μ is a convergence factor. This parameter-update law possesses many interesting statistical properties and is a proven algorithm. Its main problem is that obtaining $\nabla\xi(n)$ is often impractical and computationally intensive.

The simplest approximation to $\xi(n)$ is to use the instantaneous squared error instead. Then

$$\hat{\xi}(n) = e^2(n)$$

and the gradient used in the algorithm is

$$\nabla\hat{\xi}(n) \quad = \quad 2[\nabla e(n)]e(n) = -2\mathbf{x}(n)e(n) \tag{4.7}$$

When the estimate of the gradient in Equation (4.7) is substituted in Equation (4.6) the well-known LMS rule is obtained:

$$\mathbf{p}(n+1) = \mathbf{p}(n) + \mu\mathbf{x}(n)e(n) \tag{4.8}$$

or, if using the control scheme in Figure 4.9 and thus the error expression in (4.3), its derivation to FXLMS

$$\mathbf{p}(n+1) = \mathbf{p}(n) + \mu\mathbf{x}'(n)e(n) \tag{4.9}$$

This algorithm, as stated before, is simple, computationally inexpensive and effective. It is a good quality/price choice. One could argue, nevertheless, that its derivation was carried out in an ideal environment, with no consideration of model uncertainties or noise of any kind,

which are necessary to guarantee boundedness properties of the parameters or the errors, or even convergence of the algorithm. Two modifications were then applied to Equation (4.8), in order to fulfill this lack of real considerations: robust normalization and σ-modification.

On the one hand, robust normalization is basically used to make the algorithm independent of signal-power changes. On the other hand, σ-modification guarantees boundedness of the parameters and its derivatives and boundedness of the estimation error against modeling errors, and also convergence of the algorithm (zero error) when there is no modeling error.

Robust normalization and σ-modification are summarized in the following equations:

$$
\begin{aligned}
\mathbf{p}(n+1) &= (1 - c\sigma(n))\mathbf{p}(n) + c\epsilon(n) \\
\epsilon(n) &= K[y(n) - \hat{y}(n)] \\
K &= \frac{r(n)}{1 + m_s(n)} \\
\hat{y}(n) &= \mathbf{p}^T(n)r(n)
\end{aligned}
$$

where $r(n)$ is the regressors vector, c is related to the convergence rate and is chosen by the designer from $0 < c < 1$. The adaptive value $\sigma(n)$ plays an important role to avoid parameter drift, and it is defined as

$$
\sigma(n) = \left\{
\begin{array}{lll}
0 & \text{if} & \|\mathbf{p}(n)\| \leq M \\
\left(\frac{\|\mathbf{p}(n)\|}{M} - 1\right)\sigma_0 & \text{if} \quad M < \|\mathbf{p}(n)\| \leq 2M \\
\sigma_0 & \text{if} & \|\mathbf{p}(n)\| > 2M
\end{array}
\right.
$$

The constant σ_0 is a positive value such that $\sigma_0 < (1-c)/2$. The constant M is a bound of the Euclidean norm of the (unknown) true parameter set. M must be estimated beforehand and it allows bounding the parameters if their norm grows larger than M. The normalizing value $m_s(n)$, initialized to zero, is calculated with the following equation

$$
m_s(n+1) = (1 - \delta_0)m_s(n) + x^2(n) + y^2(n)
$$

where δ_0 is a parameter related to the frequency band, considering bounded uncertainty.

In this work, the parameters of the algorithm were set to the following values throughout all

the experiments: $c = 0.5$, $\sigma_0 = (1 - c)/4 = 0.125$, $M = 0.5$ and $\delta_0 = 0.1$.

4.2.2   Real Time Stable Identification: A Nehari/SOS Approach

Clearly for a FF solution to ANC a stable adaptive identification is needed, which in turn should be implemented in real-time [Lue34, NE92, KM95]. There, significant noise attenuation can be achieved through FB and/or FF controllers. As mentioned before, in the first case there are many well known limitations of the feedback loop that produces a poor performance. These performance limitations are mainly due to the nonminimum phase nature of the plant (see [FL85, SBG97], and also [HB98] and its revision in [FHMT03]), which in turn is derived from the time delay of sound propagation, *e.g.* acoustic tubes. Instead, a FF filter performs better because it is not restricted to the loop limitations. In this kind of application, the FF controller acts as a real time identifier of the acoustic noise signal received by the error microphone at the end of the tube, in order to cancel it at that point. Usually an adaptive identification scheme is used which can produce unstable behaviors in many situations. A complete experimental study of an hybrid – FF/FB controller applied to ANC in a tube can be found in [CMS07].

As a consequence, a convergent adaptive identifier with guaranteed stable behavior and numerical robustness is very useful in these situations. Such an algorithm is described in [GSPnM07]. Numerical stability is achieved by the use of Second Order Sections (SOS) structures, and the stability of each section is guaranteed by a stable Nehari projection ([BGR90]), which provides the nearest (optimal) stable model to a possibly unstable one. Due to the fact that the objective of this procedure is to implement it in real time situations, the Nehari projection is developed in analytical form.

Unstable Model Problems

As stated before in this work, the traditional assumptions in adaptive control (lack of perturbations or high frequency uncertain dynamics and minimum phase models) have generated at the end of the 80's an intense work in the area of robustness of adaptive laws [Tao03, Nar86, IS96]. These have been extensively studied since then, and an excellent survey in this area can be found in [OT89].

Still then in adaptive identification, the stability of the resulting IIR model is generally not guaranteed, causing serious practical problems particularly in FF implementations. There are

methods to convert IIR to FIR like the *Nehari shuffle* ([KBG92]) and a recent LMI optimal version in [YAN02], but the error is usually greater and requires a larger number of parameters in general. The use of IIR filters instead of FIR structures has the potential to decrease the identification error due to the fact that they include the poles dynamics. In addition, this class of filters are more efficient in modeling signals in certain applications and require smaller model orders ([Rao93]). Therefore an IIR filter that can guarantee a stable behavior and can be used in real time applications is a necessary tool in practical situations. As described in [GSPnM07], this can be achieved using the Nehari projection algorithm.

Numerical Problems

On the other hand, numerical problems also arise in real time applications, depending on the structural representation of the model. Take for example an 11th. order stable filter implemented with three different model structures: zero–pole (ZP), state space (SS) and transfer function (TF), the latter in terms of numerator and denominator coefficients, as follows:

$$\text{(ZP)} \quad \prod_{i=1}^{m} \frac{(z_i z^{-1} - 1)}{(p_i z^{-1} - 1)}, \quad \text{(TF)} \quad \frac{\sum_{i=0}^{m} z^{-i} b_i}{\sum_{i=0}^{m} z^{-i} a_i}$$

$$\text{(SS)} \quad \begin{aligned} x_{k+1} &= A x_k + B u_k \\ y_k &= C x_k + D u_k \end{aligned}$$

The complexity of each model is $\mathcal{O}(m^2)$ in the case of SS and $\mathcal{O}(m)$ in the other two cases, therefore from this point of view, the ZP and TF structures are more efficient. Nevertheless, it is a well known fact that the pole locations in the case of the TF structure, particularly in high order models, are significantly modified, even producing unstable poles ($|p_i| > 1$), as illustrated in Table 4.1. On the other hand, it is easier to use the TF representation as the difference equation which implements the filter in real time, as follows:

$$y_k = \frac{1}{a_0} \quad \begin{aligned} [b_0 \, u_k + \cdots + b_m \, u_{k-m} \\ -a_1 \, y_{k-1} - \cdots - a_m \, y_{k-m}] \end{aligned} \tag{4.10}$$

Therefore, the TF representation has advantages in terms of complexity and implementation, but serious disadvantages in terms of perturbations of pole locations, at least in high order models.

The solution to this problem is obtained by a series connection of SOS', which is an adequate

ZP	SS	TF
0.0034	0.0034	0.0034
0.9975	0.9975	1.0295
0.9975	0.9975	1.0295
0.9949	0.9949	1.0128
0.9949	0.9949	1.0128
0.9607	0.9607	0.9924
0.9608	0.9608	0.9924
0.9802	0.9802	0.9646
0.9995	0.9995	0.9646
0.9995	0.9995	0.9434
0.9961	0.9961	0.9434

Table 4.1: Absolute value of poles of a discrete–time system represented in
zero–poles (ZP), state–space (SS) and transfer function (TF).

way of implementing filters in real time. The SOS structure is numerically more efficient than
the plain TF structure due to the fact that it has 2nd. order numerator and denominator, there-
fore preserving the original pole–zero locations. In addition, cascade-forms of SOS provide
an attractive realization for adaptive IIR filters because the stability of the filter parametriza-
tion is easily monitored, and because filter pole locations are readily obtained from the adapted
parameters with low computational cost ([WAN95]).

In the previous example, the SOS' pole locations coincides with the ZP and SS structures.
Furthermore it is still $\mathcal{O}(m)$ and each SOS can be implemented as a difference equation con-
nected in series with all other SOS', as follows:

$$\frac{Y(z)}{U(z)} \;\; = \;\; \prod_{i=1}^{m/2} \frac{z^{-2}b_2^i + z^{-1}b_1^i + b_0^i}{z^{-2}a_2^i + z^{-1}a_1^i + 1} \tag{4.11}$$

where each SOS correspond to a 2nd. order difference equation of the form

$$y_k^i \;\; = \;\; b_0^i \, u_k^i + b_1^i \, u_{k-1}^i + b_2^i \, u_{k-2}^i - a_1^i \, y_{k-1}^i - a_2^i \, y_{k-2}^i$$

where $a_0^i = 1$ for simplicity.

(a) (b)
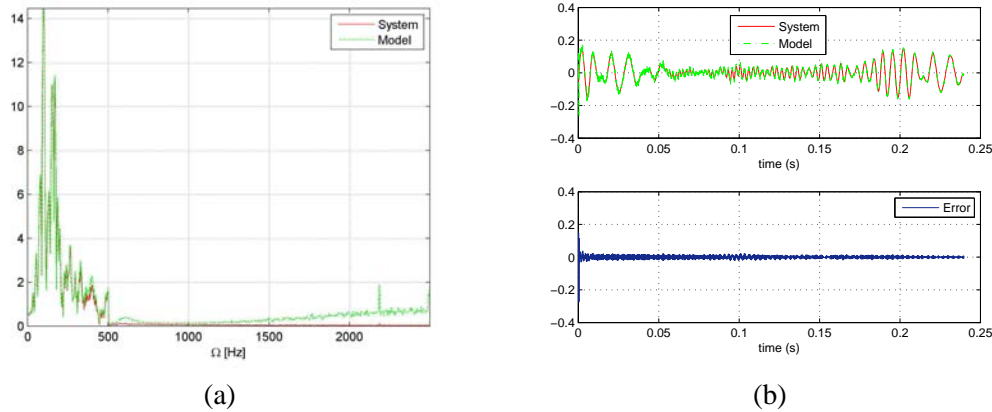
Figure 4.7: Secondary circuit: (a) 12th. order experimental data approximation - time response. (b) 12th. order experimental data approximation - frequency response.

Application Examples

Example 1. The present and the next practical examples are taken from measurements in an acoustic duct in an ANC experience. The duct is described in Chapter 3. The input signal is produced by an industrial fan and has been measured by the reference microphone located next to it. The output signal has been measured by the error microphone at the other end of the tube, therefore the primary circuit is identified. The identification scheme is based in the Projection algorithm ([Tao03]) and the initial coefficients of all SOS sections have been computed from an off-line identification of the complete transfer function based on a parametric- nonparametric technique ([PSS99]). This is a convenient practical approach so that the algorithm is initiated from a close enough neighborhood of the actual parameters. The off-line identification procedure can be anyone which can produce a sufficiently good model of the experimental data, taking advantage of the fact that it does not need to be implemented in real time. The results are presented in Figures 4.7, which evidence a good fit of the experimental data, both in frequency and time.

Example 2. This example considers experimental data generated by the same duct, but with the control speaker as the main noise source producing a multi–sinusoidal signal. The output is again obtained from the error microphone. The system to be identified is now the secondary circuit based on a high order model (40th). Again, a previous off-line identification has been made by means of a parametric–nonparametric robust identification algorithm in [PSS99]. The
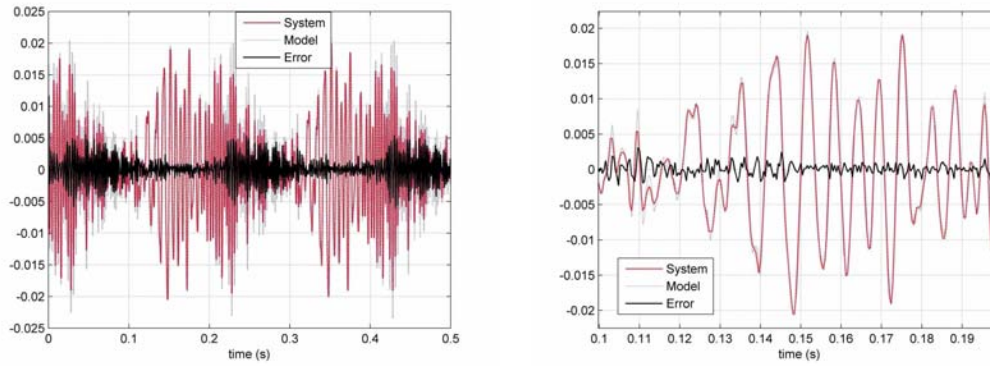
Figure 4.8: 40th. order experimental data approximation.

online identification scheme is again based on the Projection algorithm and has considered the first 500 data points. The remaining 1000 data points are used as a validation test. Here the main objective is to test the algorithm against numerical errors produced in cases where high order models are used. The fit is good enough and the error is bounded, as shown in Figure 4.8.

CHAPTER 5

FEEDBACK CONTROL STRUCTURES

The main objective approached in this chapter is to apply robust (control oriented) identification to an ANC system, with a deterministic worst-case criteria in order to design a robust controller. Based on the experimental knowledge of low frequency modes, a parametric/dynamic model identification method [PSS99, BMS01] is applied. This produces a multiplicative global uncertain set to describe the physical plant, which exactly fits the robust controller design framework. This is applied to an actual duct using two different noise sources: a speaker and a fan. Theoretical and experimental results are presented and the resulting experimental performance is comparable or even better than other robust methods applied to ANC.

5.1 Parametric/Dynamic Robust Identification

Here a systematic procedure that covers the experimental data by a model set is presented. The data fed to the identification algorithm used to identify the model of the secondary circuit $G_{sec}(z)$ and the performance weight $W_p(z)$ is as follows (see Figures 3.4(a) and 5.1):

- Time signal measured at the error microphone which picks up the acoustic signal from the noise source to identify the primary circuit's main perturbing frequencies.

- Input a DSP multi–sinusoidal (time) signal commanded to the control speaker, and read the error microphone signal, to identify the secondary circuit.
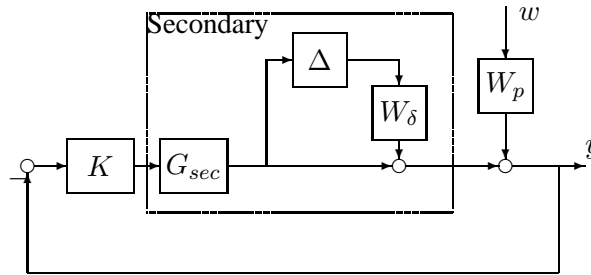
Figure 5.1: Feedback (FB) design setup, with primary circuit perturbation
(W_p) and secondary model with multiplicative uncertainty.

The input and output time signals are converted to frequency domain information *via* an FFT. The frequency response data is obtained by dividing these signals –output over input. The sampling time is $T_s = 0.2$ ms, and 500 Hz is the maximum input frequency to the system. Therefore above 500 Hz this quotient has a large numerical error due to the fact that both signals are almost zero there, hence it is filtered. The periodicity of the FFT is theoretically 1000 samples, and each experimental run has $2 \cdot 10^4$ samples, *i.e.* 20 sets. The average of these sets is taken as the nominal experimental data and its deviation shows a reasonable short term repeatability. In addition, measurements from one day to another also confirm a repeatable experiment.

The identification procedure can be found in [PSS99, BMS01], and combines both parametric and dynamic models using time and/or frequency experimental input data. It is computed solving a set of LMIs using the Toolbox in [MPS04]. This in turn is based on a general rational interpolation theory developed in [BGR90], which combines classical frequency response (Nevanlinna–Pick) and time response (Carathéodory–Fejér) interpolation results.

It is a fact that the model order in classical interpolation duplicates the number of data points, in the case of frequency data. Hence, the use of parametric second order models to fit the most significant frequency peaks corresponding to the different modes appearing in the duct (see [HAV[+]96]), drastically reduces the model order. Therefore, the remaining part of the plant can be suitably interpolated by a nonparametric dynamic model. This is valid not only in this application but in any other problem where well defined peaks are present in the experimental data, *e.g.* mechanical flexible structures, aeroelasticity.

The class of *a priori* models and measurement noise sets considered are in the framework presented in [PSSI98]. They correspond to exponentially stable systems (finite or infinite dimensional) that satisfy the time domain bound $|h(k)| \leq K\rho^{-k}$, defined by parameters $K < \infty$ and $\rho > 1$. The frequency and time domain noise sets are defined by hard bounds ϵ_f and ϵ_t, respectively:

$$\mathcal{N}_f \;=\; \left\{ \eta^f \in \mathbb{C}^{N_f}, \;\; |\eta_k^f| \leq \epsilon_f \right\}, \quad \mathcal{N}_t = \left\{ \eta^t \in \mathbb{R}^{N_t}, \;\; |\eta_k^t| \leq \epsilon_t \right\}$$

The experimental data are N_f (N_t) samples of the frequency (time) response of the system at frequency (time) values Ω_k (t_k), corrupted by noise realizations belonging to the sets previously defined. The frequency (time) noise bounds are based on the experimental setup. The parametric information is fitted by means of a finite set of Kautz orthonormal basis $B_i(z)$ tuned to the experimental information as shown in [BMS01]. This is supported by the modeling results for these type of applications, as explained in [HAV$^+$96]. The resulting identified model has the form:

$$H_{id}(z) \;=\; H_{np}(z) + \sum_i^N p_i B_i(z)$$

The optimization procedure interpolates, within the error bounds, simultaneously the dynamic portion $H_{np}(z)$ and the parameters $\{p_i, \;\; i \;=\; 1, \ldots, N\}$, such that consistency[1] is achieved. It is solved *via* a set of LMI's, hence it is convex. Figure 5.2(a) illustrates the fitting of the 2nd order Kautz bases to the experimental information from a duct. The number of peaks to be fitted depends on the particular application and is related to the frequency range where performance should be guaranteed. Figure 5.2(b) shows the selected interpolation points, 5.2(c) the parametric and dynamic components and model error of the secondary acoustic circuit, and in Figure 5.2(d) the resulting identified model.

From Figure 5.2(c) it seems that the secondary model error could be sufficiently small to provide a representative nominal model to design a controller. Nevertheless, the significance of the model error depends on the use it will have, the resulting model order, and the performance frequency range of interest. This is discussed next:

---

[1]A model is consistent if it can reproduce the experimental data within the sets of model and noise *a priori* information.
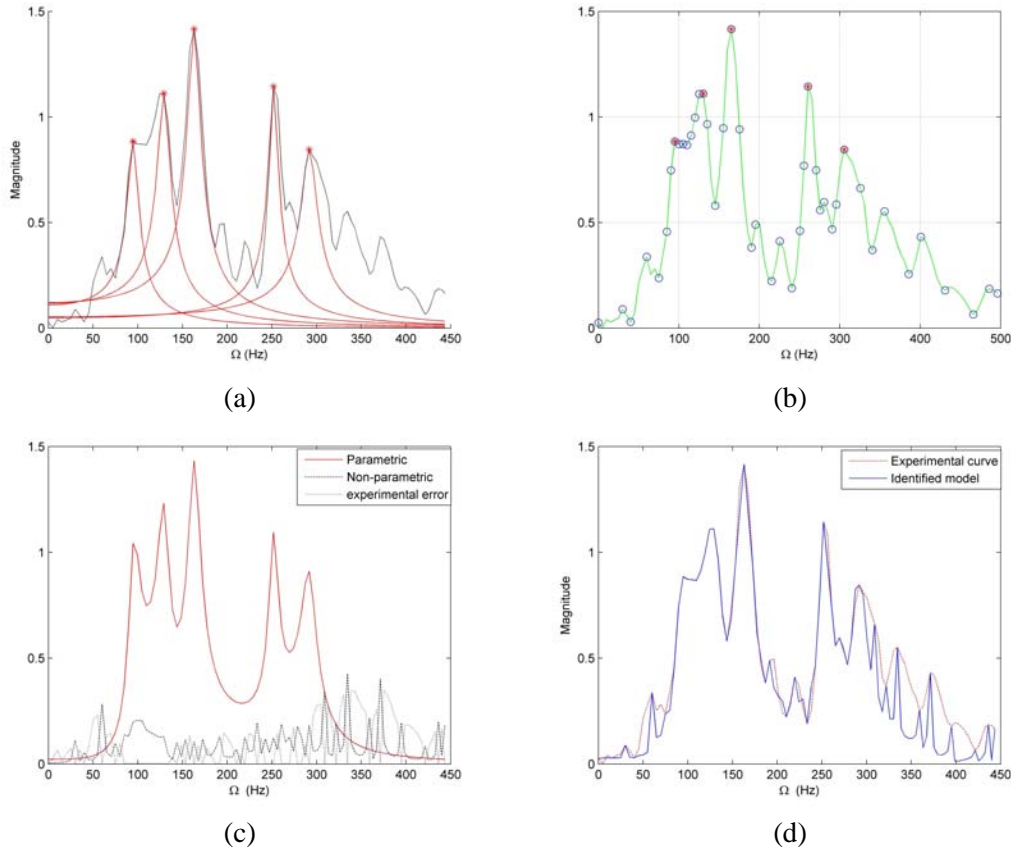
Figure 5.2: Secondary circuit: (a) Kautz bases fitting, (b) interpolation
points, (c) parametric, dynamic and model error, (d) identified
model.

Primary: In a feedback (FB) scheme (see Figures 3.4(a) and 5.1), the primary model combined
with the frequency response of the noise source provides a perturbation signal at the input of the
error microphone. Here only an approximate weight W_p is needed (see Figure 5.3(b)), which
emphasizes the main disturbing frequency bands where performance is required. Hence, the
order can be kept small, so that it does not significantly increase the controller order. In any
case, the efficiency of the weight in recovering the important frequency range is verified at the
end *via* the robust performance analysis.

Secondary: This model is used in the FB loop, and if the plant is represented by a multiplicative
uncertain set of models, the *relative* or *multiplicative* error is important, due to the fact that
both, robust stability and performance depend on the value it takes. This relative error is the

(a)   (b)
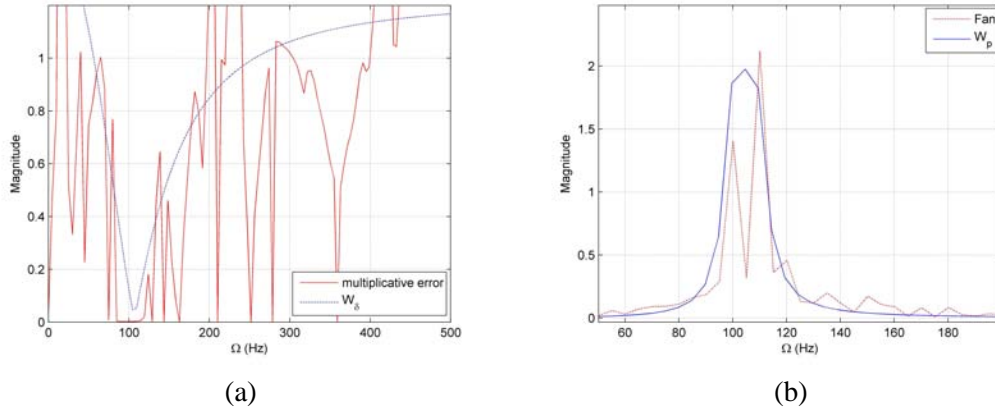
Figure 5.3: (a) Uncertainty weight and multiplicative identification error,
(b) frequency response of the error microphone output with the
fan as the noise source, covered by the performance weight W_p.

(additive) error illustrated in Figure 5.2(c) divided by the experimental data in Figure 5.2(d), frequency by frequency, which produces the curve in Figure 5.3(a). This can take very high values at points where the magnitude of the experiment is near zero, *e.g.* at low frequencies[2]. For design purposes, this error is "covered" by a weight W_δ, also in Figure 5.3(a). The model order of this weight increases the controller order, therefore it should be limited. Finally, the fit of the secondary model G_{sec} in Figure 5.2(d) seems good enough, but its order is 96: too high to design a feedback controller which should run in real time with the available hardware. Not only real time implementation, but also numerical errors are a potential source of errors. As a consequence, in this application the identification stage is performed taking these practical problems into consideration.

5.2   Robust Controller Analysis and Design

This section applies standard results in [DFT92, ZDG96, SS98] to this problem. The control objective is to minimize at the error microphone output, the effect of the (acoustic noise) disturbances due to the noise source passing through the primary circuit. Therefore, a practical

---

[2]Considering additive uncertainty does not help, because the inverse of the nominal model still appears in the robust stability test: $\|W_{add}(z)G_{sec}^{-1}(z)T(z)\|_\infty = \|W_\delta(z)T(z)\|_\infty < 1$.

approach is to model the disturbance as a *set* of signals $w(t)$ in a certain frequency range, represented by weight $W_p(s)$ (see Figure 5.1). If the energy of signal $y(t)$ at the error microphone is to be minimized, the approach from a worst case perspective, is to consider *all* disturbances $w(t)$ in the set. In addition, the system is represented by a global dynamic (multiplicative) set of models: $\mathcal{G} \triangleq \{[1 + W_\delta(z)\Delta]\,G_{sec}(z),\ |\Delta| < 1\}$, which is a practical description of uncertainty which does not require structured *a priori* knowledge of the plant, *e.g.* model order, and leads to convex optimization solutions. The final objective is robust performance which solves both problems simultaneously with the same controller. Necessary and sufficient conditions to meet nominal performance (NP), robust stability (RS) and robust performance (RP) are, respectively:

$$\text{NP} \iff \|y\|_2 \le 1, \quad \forall \|w\|_2 \le 1 \iff \|S(z)W_p(z)\|_\infty \le 1 \tag{5.1}$$

$$\text{RS} \iff \|T(z)W_\delta(z)\|_\infty \le 1 \tag{5.2}$$

$$\text{RP} \iff |T(z)W_\delta(z)| + |S(z)W_p(z)| \le 1, \quad \forall z = e^{\jmath\Omega T_s} \tag{5.3}$$

The robust performance condition coincides with the μ (semi-)norm for this SISO problem. Here $S(z)$ and $T(z)$ are the sensitivity function and its complement, and $\|\cdot\|_2$ represents the energy of the signal. For practical reasons, instead of using μ-synthesis, the design is solved as a mixed sensitivity problem using $\mathcal{H}_\infty$ control, because it produces a lower order controller.

$$\min_{i.s.K(z)} \left\| \begin{bmatrix} T(z)W_\delta(z) \\ S(z)W_p(z) \end{bmatrix} \right\|_\infty \tag{5.4}$$

Here $i.s.$ stands for internally stabilizing controllers. Both the performance W_p and the robustness W_δ weights are related to the performance specifications and identification data of the problem, respectively. The reasoning behind the weight selection is as follows.

The performance objective is to decrease the sensitivity of the system at the main frequencies of the signal coming from the primary circuit. The combination of primary circuit's and noise source frequency responses have the main peaks in the range $[95, 115]$ Hz, as can be observed in Figure 5.3(b). Therefore, $W_p(z)$ has been selected such that it increases the performance at those frequencies as illustrated in the same figure. The robustness weight $W_\delta(z)$, has been obtained so that it "covers" the multiplicative error frequency response, particularly in the range where performance is needed (see Figure 5.3(a)).

From a practical standpoint, the robust performance condition (5.3) could be modified by replacing the uncertainty weight $W_\delta(z)$ by the actual frequency magnitude of uncertainty (full

(a)

(b)

(c)

(d)
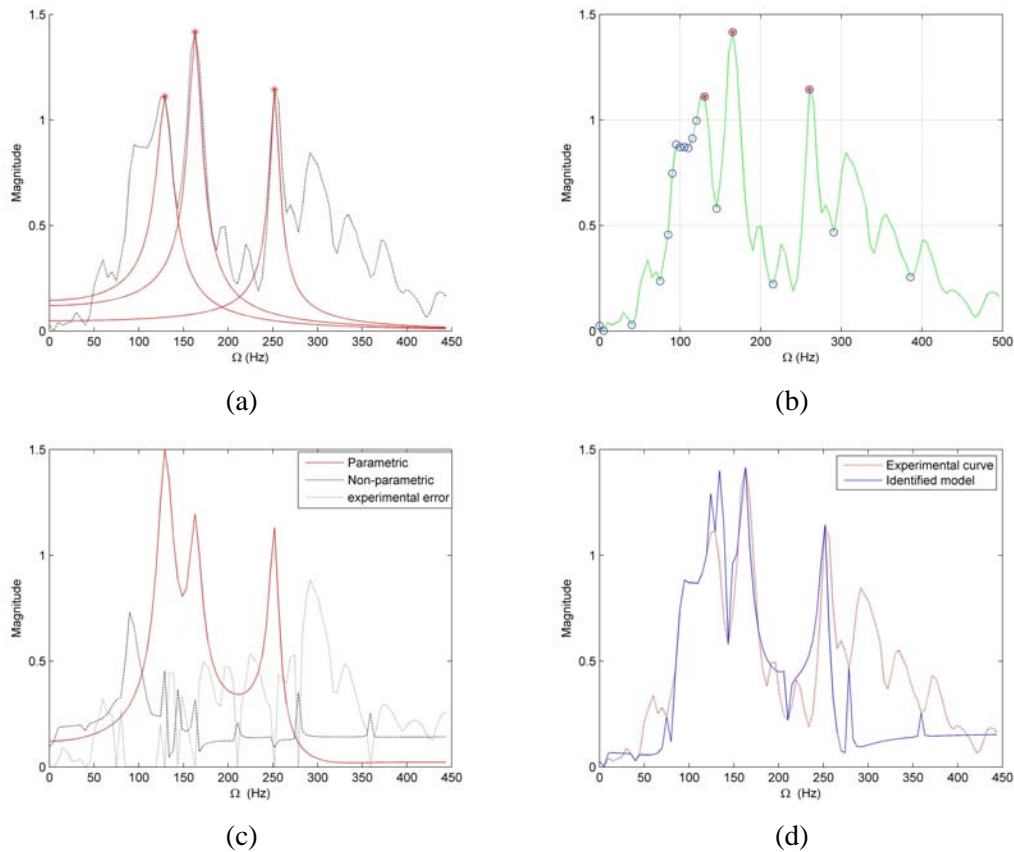
Figure 5.4: Secondary circuit: (a) less Kautz basis, (b) less interpolation
points concentrated in performance region, (c) parametric,
dynamic and model error, (d) identified model.

line in Figure 5.3(a)). Hence, the design would still use the weight $W_\delta(z)$, but the analysis
condition would be more realistic by using the actual multiplicative error. Another practical
issue is actuator saturation, which could be considered in the design procedure. Special attention
to this kind of practical issues will be given in Section 6.2.

5.3   Main Results

5.3.1   Identification preliminaries

Due to practical compromises related with model order and performance bandwidth (explained further in section 6.2, in a compendium of practical compromises which arise in the robust identification and controller design stage for ANC systems, and its solutions) the order of the nominal model has been decreased by eliminating interpolation points and concentrating them in the important "performance" bands. The fit of the secondary model G_{sec} in Figure 5.2(d) seems good enough, but its order is 96: too high to design a feedback controller which should run in real time with the available hardware. Not only real time implementation, but also numerical errors are a potential source of errors. As a consequence, in this application the identification stage is performed taking these practical problems into consideration. The multiplicative iden-tification error restricts not only RS, but also performance robustness. Therefore, it should be decreased only in the regions where higher performance is needed, i.e. at the "performance" range pointed out previously. This has been solved by adding more interpolation points in this frequency range, keeping the total number of points as low as possible not to increase the order (compare Figure 5.4(a) with 5.2(a)). This is a way of keeping track of the relation between robustness and performance as well as the order of the controller at the identification stage, instead of only reducing the order of the controller at the end of the design. In addition, the number of Kautz basis have been reduced from five to three, for the same reason. If necessary at the end, a balanced model order reduction step can be applied to the controller, based upon its Hankel singular values. According to the previous comments, a new identification iteration was carried out for the total design. Previously, 44 interpolating points (order 86), plus 5 Kautz basis (order 10) resulted in a 96th order nominal model (see Figures 5.2(a) to 5.2(d)). Instead, a new identification was performed with 3 Kautz basis and only 20 interpolation points (Figures 5.4(a) and 5.4(b)), producing a 44th order model (Figures 5.4(c) and (d)). Note that this model does not fit the experimental data as well as the previous one, but now it has a much lower order. The identification (additive) error in Figure 5.2(c) is much lower than the one in Figure 5.4(c), which can also be seen by comparing Figures 5.2(d) with 5.4(d). Now, the identification has been concentrated in the frequency range $[95, 115]$ Hz and as a consequence, the multiplicative error is better in this "performance" band, as illustrated in Figure 5.3(a). Nevertheless, note that at frequencies above 200 Hz the weight W_δ does not cover the multiplicative identification error. To achieve this coverage, a higher order weight could have been considered, which in turn
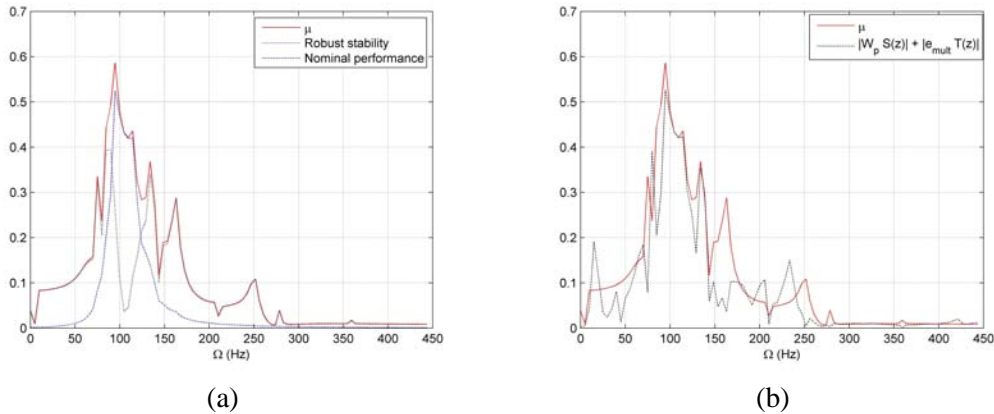
Figure 5.5: (a) Structured singular value robust performance analysis, (b) practical robust performance analysis.

would have increased the controller order. Instead, weight W_δ in figure 5.3(a) was used in the design stage, but the multiplicative identification error in the same figure (dashed) replaced W_δ in condition (5.3), for the robust performance analysis. This provides a more practical analysis condition.

The controller was designed using the weights in Figure 5.3. After a balanced realization and state truncation, based on its Hankel singular values, the order was reduced to 15. The theoretical and experimental results are compared in the next section.

5.3.2 Experimental Results

In this section, theoretical and experimental results are compared. Two noise disturbance signals were applied: an industrial fan (see Figure 3.1), and a speaker located at the same place as the fan but excited by a signal generator. The frequency response of the fan through the primary circuit measured by the error microphone can be seen in Figure 5.3(b), and the relevant frequencies that perturb the output of the tube are around 100 and 105–110 Hz. The actual fan could have possible nonlinearities and/or time variations that have not been taken into account in the LTI[3] statement of the problem. The speaker is used instead to produce noise in the [95,115] Hz band and provides a more controllable (as well as ideal) experimental setup, producing similar

---

[3]Linear Time Invariant.
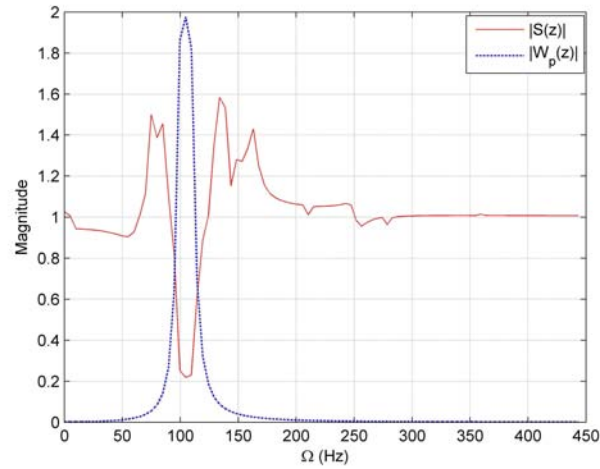
Figure 5.6: Sensitivity function and performance weight.
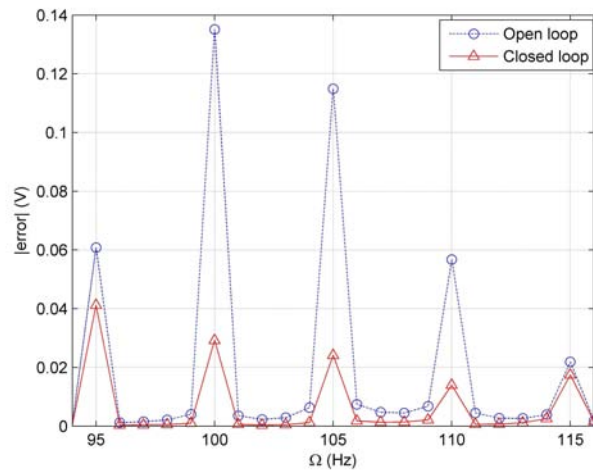
Figure 5.7: Controlled (triangle) and no control (circle) frequency
response: Speaker.

conditions as the ones in the identification experiments.
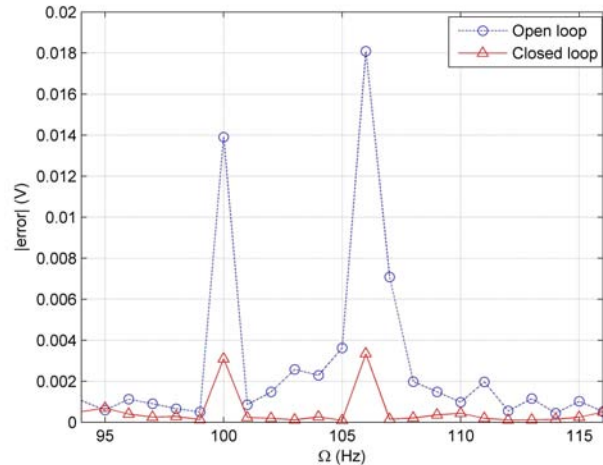
Figure 5.8: Controlled (full) and no control (dashed) frequency response: real fan.

The theoretical analysis is presented in Figures 5.5(a) and (b). In the first one, nominal performance, robust stability and the robust performance test in Equation (5.3) are compared. As indicated previously, the latter coincides with the optimal measure provided by the structured singular value μ in this case, due to the fact that the system is SISO. These are all below unity, therefore the design guarantees robustness and performance simultaneously. Nevertheless, due to the fact that the actual uncertainty is not covered at all frequencies by the uncertainty weight W_δ (Figure 5.3(a)), a slightly more practical analysis condition has been considered, as commented in section 5.2. In Figure 5.5(b), the magnitude response of the actual relative uncertainty of the model (the multiplicative error in Figure 5.3(a)) replaces the weight W_δ in the robust performance condition (5.3). This new condition is still below one which provides more practical guarantees of robust stability and performance.

Note that the robust performance condition could have been pushed near to one, therefore increasing performance. This was attempted as a new design, and performance in the $[95, 115]$ Hz bandwidth was therefore increased to around 18 dB of attenuation. Nevertheless this controller also produced an excessive amplification at $f = 65$ Hz, that although outside the region excited by the speaker and the fan, still produced an audible disturbing noise. This is a clear consequence of the *waterbed* effect, where theory predicts an amplification of frequencies outside this bandwidth as shown in Figure 5.6. Therefore, the previous design was left with the resulting

	100 Hz	105 Hz	110 Hz	[95,115] Hz
Theory	12 dB	13.2 dB	11.5 dB	13.2 dB
Speaker	13.3 dB	13.6 dB	12.15 dB	10.3 dB
Fan	13 dB	14.6 dB (@106 Hz)	—	14.3 dB

Table 5.1: Feedback controller performance (attenuation) comparison.

performance presented in Table 5.1.

Performance is measured as the controlled (closed loop) over the uncontrolled (open loop) attenuation. It can be theoretically predicted using the magnitude of the sensitivity function at the relevant frequencies mentioned previously, as illustrated in Figure 5.6. In practice instead, the performance of the speaker and fan experiments are calculated as the quotient between the energy of the signals at the error microphone, in closed and open loop, respectively. These results are presented in Table 5.1. The attenuation between controlled and uncontrolled behaviors for both experiments are also illustrated in Figures 5.7 and 5.8, which compare magnitudes instead of dB's for clarity of presentation.

The Table presents the attenuation at the most relevant peaks, in this case $100, 105$ and 110 Hz, as well as the attenuation in the whole bandwidth. Note that the theoretical values have a good match with both experiments. The experiments with the fan were not as "clean" as the ones with the speaker, due to a slight nonlinear and/or time varying behavior, possibly explained by a variable rotation speed and/or atmospherical changes (*e.g.* temperature, humidity). For this reason, the controller was tuned to perform better in the whole bandwidth $[95, 115]$ Hz, and not only at the main peaks amplified by the fan: 100 and 106 Hz. Experiments performed in different days with the same fan showed a (slow) shift in these peaks, but always inside the relevant bandwidth. This is also the reason why experiments with a speaker that had a clear LTI behavior for all experimental outcomes have been performed.

Finally some comments on the overall match between theory and both experiments. Theoretical results assume a certain amount of uncertainty in the model, in order to guarantee both stability and performance for *all* models in the global dynamic (multiplicative) set, *i.e.* robustness. Note that the uncertainty weight, particularly in the relevant frequencies, does not cover tightly enough the *actual* uncertainty curve (see Figure 5.3(a)). The slight conservatism introduced by this coverage was at the expense of not increasing the weight's order and hence the controller order. The resulting performance depends on how near the actual plant is to the

nominal model (higher) or to the *worst case* model (lower). The same happens with the set of disturbances $\{W_p(s)w, \ \|w\|_2 \leq 1\}$, where for every element in the set, a different performance is obtained. In both cases, $\mathcal{H}_\infty$ control designs for the worst model and disturbance in both sets, but the actual result depends on *what* model and disturbance really occurs. This is a partial explanation why the theoretical, fan and speaker overall performances differ from one to another.

Finally, the overall experimental performance is comparable or even better than other works in the area. Next steps consider general hybrid (FF/FB) control structures and sensor and actuator locations as part of the control design problem. Research concerning these areas will be shown in Chapter 6 and Chapter 7. Moreover, in Chapter 6 the compromises between identification and control in a practical ANC situation will be also discussed in detail.

CHAPTER 6

HYBRID (FEEDFORWARD/FEEDBACK) STRUCTURES

In this chapter, an hybrid (FF/FB) controller is designed to cancel the acoustic noise in the duct described in Chapter 3. Furthermore, the compromises and practical issues which arise in the robust identification and controller design stages for an ANC system are explicitly pointed out. These are mainly derived from the compromises between identification and control, performance and robustness, feedback limitations, model and controller order, and implementation issues.

The control system has a FULMS control structure as shown in Figure 4.6, which has been explained in greater detail in Section 2.2 and Section 4.1. This structure avoids the use of unstable filters for the cancelation of the nonminimum phase zeros of the secondary path, and compensates the acoustic feedback. The FF controller is based on the robustly normalized σ-algorithm and is adaptive in nature (see Section 4.2.1), and the FB is an $\mathcal{H}_\infty$ optimal controller (see Section 5.2). Due to changes in the structure of the experimental plant (Figure 3.1) from experiments in Chapter 5, a complete new process of system identification and design of the FB controller has been performed in this chapter.

6.1 Experimental Results

The controllers have been tested with three input noise sources (see Chapter 3):
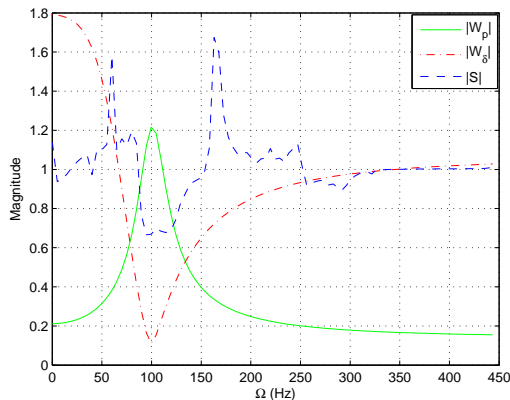
Figure 6.1: Uncertainty (W_δ), performance (W_p) weights and sensitivity
function S for the synthetic-fan experiment

Structure	Order	Single tone	Synthetic fan	Industrial fan
FF	30	81.25 dB	9.56 dB	7.56 dB
FB	12	3.90 dB	4.15 dB	3.82 dB
Hybrid	30+12	82.36 dB	12.72 dB	10.1 dB

Table 6.1: Experimental characteristics and attenuation for different control
structures

- A speaker-generated single-frequency tone of $\Omega = 105$ Hz.

- A speaker-generated synthetic fan with bandwidth $\Omega \in [95, 115]$ Hz.

- The actual industrial fan.

The results are presented in Table 6.1. The hybrid design was also tested with the real fan
and shows a good agreement with the synthetic test (see values in the same table). Figures 6.2,
6.3 and 6.4 compare the open-loop and closed-loop responses for the three different input noise
sources, respectively. Figure 6.5 shows the attenuation attained by the hybrid (FF/FB) controller
with the three different input signals. The attenuation values for the actual and the synthetic fan
correspond to the performance bandwidth of interest.

Some comments on these results are pointed out next. The FF controller performs much better for a single tone. This seems less demanding for the adaptation algorithm than a set of different tones, for which the performance decreases significantly. Nevertheless, in this last case where a finite bandwidth is applied, the results are similar for both the synthetic and industrial fan.

The FB controller has clear performance limitations, mainly due to the nonminimum phase zeros, hence it does not perform as well as the FF. It has been designed based on a (conservative) set of models that represents the actual plant. This explains why this robust controller performs similarly for all inputs. Only with more information on the real fan, *i.e.* less uncertainty and a smaller model set, could the controller have performed better, probably with the extra cost of a higher order. Another step to increase performance would be to include the fan's nonlinear/time-varying characteristics in the model and uncertainty descriptions, and design a nonlinear controller.

In the same table, there is a good agreement in the attenuation produced by each controller separately, and combined together in an hybrid structure for all three inputs, *i.e.* the sum of both values add up to approximately the attenuation for the hybrid control. Although this design approach was tuned to the synthetic signal, it performs very well when applied to the real fan, as indicated in Table 6.1. This result can be justified by the fact that model uncertainty covered both, synthetic and real fans, in the same set.

6.2 Compromises and Discrepancies between Theory and Practice

6.2.1 Practical Compromises and Solutions

Besides maximizing performance and robustness, it is important to consider several practical constraints. They generate compromises in the controller design and possible identification iterations. These compromises arise from different sources: (i) feedback-loop constraints (see [FL85, SBG97], and in particular for ANC, see [HB98]), (ii) identification and control design interplay, (iii) implementation issues. These practical problems, which impose constraints in this application, are enumerated altogether next.

1. The nominal model of the secondary path has right half-plane zeros that limits performance in the FB case.

2. Frequency interpolation is used as an identification tool, therefore the model order is directly related to the number of interpolation points.

3. The usual robustness/performance compromise is a direct consequence in this case of Equation (5.3). This, in addition, forces an identification/control compromise, *i.e.* the multiplicative identification error should be lower than one in frequencies where noise attenuation (performance) is needed.

4. An additional problem is added related to the previous point. At certain frequencies where the magnitude of the model is small, the relative identification error increases; sometimes above unity.

5. Performance and robustness design weights increase the order of the augmented plant's model and therefore, of the controller.

6. The FB controller usually has poles very close to the unit circle in the design stage, which may lead to instability in the implementation, due to numerical issues.

7. The simplest way to represent the FB transfer function for controller implementation is numerator/denominator polynomials. This may lead to important pole distortion when it is implemented, specially with high-order polynomials.

8. Actuator saturation should be taken into account.

9. DSP implementation and sample time impose limitations on FF and FB controller orders.

Next, some solutions adopted in this application for the previous compromises are enumerated.

- Nonminimal phase models restrict performance in a well-known way. In fact they suffer from the *waterbed* effect, pointed out in [FL85, SBG97], which determines lower bounds in the size of the peaks of the sensitivity function magnitude $\left| S(e^{\jmath \Omega T_s}) \right|$. It is clear from here that the lower the sensitivity will be in certain frequency bands, the higher it will increase in others. Hence, the performance weight $W_p(z)$ should reflect a decrease in the sensitivity **only** at frequency bands with the highest peaks of the error microphone output, *i.e.* in the range in $[95, 115]$ Hz. This frequency band, also called the "performance"

range, determines the frequencies in which the sensitivity is below one, as indicated by Equation (5.1). The *waterbed* effect can be seen in Figure 6.1, where clearly the sensitivity is below one, and hence there is disturbance attenuation, only in the "performance" range $[95, 115]$ Hz. Instead, the controller will amplify signals with frequency content outside this range. This is not a problem when these signals have a small magnitude there, as illustrated in this case by the fan signal in Figure 6.6.

- From Equation (5.3), it is clear that only at frequencies where the multiplicative identification error is below one can robust performance be achieved. Therefore, $W_\delta(z)$ should be decreased as much as possible (while still bounding the relative identification error) *only* in frequencies where attenuation is needed, *i.e.* at the "performance" range pointed out previously. This has been solved by adding more interpolation points in this frequency range, keeping the total number of points as low as possible to avoid increasing the order. This is a way of keeping track of the relation between robustness and performance, as well as the order of the controller at the identification stage, instead of only reducing the order of the controller at the end of the design.

- The order of the nominal model may also be decreased by eliminating interpolation points and concentrating them in the important "performance" bands, as similarly done in Chapter 5. If necessary at the end, a balanced model order-reduction step can be applied to the controller, based upon its Hankel singular values.

- The relative identification error applied to the nominal model of the secondary path $G_{sec}(z)$ in Figure 5.1, could be larger at frequencies where $\left|G_{sec}(e^{j\Omega_k})\right|$ is small. To decrease it, either the nominal model can be changed locally or the noise set (and hence the identification error) can be made frequency dependent. In the latter case, the identification error bound ϵ_f^k is weighted to make it directly proportional to $\left|G_{sec}(e^{j\Omega_k})\right|$.

- The orders of both weights, W_p and W_δ, have been kept as low as possible, while taking into account the performance and robustness features pointed out previously. For example, they have been chosen as follows:

$$W_p(z) \;=\; 0.1776\frac{z^2 - 1.464z + 0.538}{z^2 - 1.869z + 0.931} \tag{6.1}$$

$$W_\delta(z) \;=\; 0.978\frac{z^2 - 1.914z + 0.9756}{z^2 - 1.775z + 0.8086} \tag{6.2}$$

and illustrated in Figure 6.1.

- The FB controller has been finally implemented rescaling the magnitude of the poles closest to the unit circle, to avoid controller fragility. Clearly, this modifies the dynamics of the controller, therefore the analysis to assure robust performance must be rechecked. The analysis figures presented in this chapter were obtained using the implemented nonfragile FB controller.

- The previous controller was implemented using a series connection of SOS, which are numerically more efficient than the polynomial representation (see Section 4.2.2).

- Actuator saturation could be taken into account at the design stage by considering an extra weight at the controller's output. In this case, due to the fact that there was no clear saturation problem, the controller action was evaluated at the analysis and implementation stages, to avoid increasing the order of the augmented design model, and hence of the controller. According to the experimental results, the controller action was well within saturation limits.

6.2.2   Discrepancies between Theory and Practice

As stated before, ANC is an active area of research and many different applications have been attempted, *e.g.* industrial and air-conditioning ducts, high-energy transformers, helmets, windows and airport surroundings. The main practical and commercial approaches consider linear models and adaptive FF solutions. There are clearly still many practical issues to be solved, for which more applied theory has to be developed. These issues increase when considering 3D environments like boxes, cabinets or even outdoor situations. A nonexhaustive list of the main issues that arise in this particular application, is presented next.

- Stability and robustness issues in adaptive FF controllers should be carefully considered. In practical situations, stability can be a potential (and fundamental) source of problems. Nonconservative nonlinear analysis tools should be used to solve this problem, so that stability and performance guarantees could be given.

- Control-oriented identification with a worst-case deterministic error bound that fits robust design methods can be very conservative in general. In the present case, the robust identification procedure used a local (experimental) identification error, instead of the global error. The more detailed the description of the system, the better performance the controller can obtain. Therefore, structured uncertainty, nonlinear and/or time-varying information

could improve the system's description and hence the resulting performance. Very limited results have been developed for nonlinear and/or time-varying system identification with a worst-case deterministic error, *e.g.* [SM03, MS04].

- High relative modeling errors (multiplicative uncertainty) in frequencies where the experimental data has smaller absolute values, clearly limits robust stability and, as a consequence, the achievable robust performance at these frequencies. Control-oriented identification could consider this problem as part of the procedure to obtain the nominal model, as a way to minimize the uncertainty in certain frequency bandwidths.

- Controller order has to be limited due to its practical real-time implementation. Model order-reduction methods, as the ones based on Hankel singular values or using frequency-band weighting, are applied. At the different stages of the identification and controller design, there are instances where controller order can be limited, *e.g.* selection and number of interpolation points, number of Kautz bases, order reduction of nominal model and weight-order selection. A clear analysis on how to decide on each instance could be very practical. In addition, design methods that consider the controller order as part of the formulation, would decrease the number of design iterations.

- Controller implementation is also an important issue, which could destroy the theoretical performance and robustness result. Numerical precision problems can arise (see Section 4.2.2), which produce a gap between the controller design and its implementation, derived in an internally fragile controller. Problems such as digital filter poles too close to the unit circle or pole distortion using numerator/denominator high-order polynomials, can be solved if they are taken into account at the design stage. To this end, numerically robust representations, *e.g.* series connection of SOS, can be used to implement the controllers in the DSP or microcomputer. Tools to take these numerical issues into account and avoid controller fragility, should be considered.

Sensor and actuator allocation should be part of the identification and controller design, similarly to what has been done in aircraft design. This could provide a global optimization design environment and would certainly relieve some of the present limitations. Some work in this area is presented in Chapter 7.
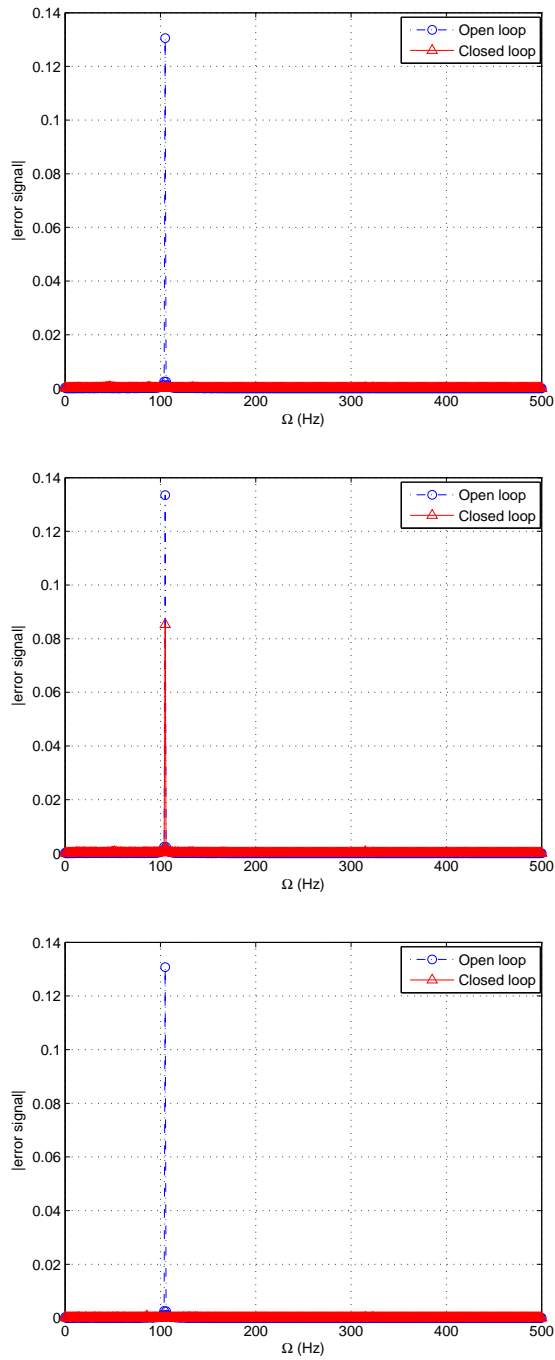
Figure 6.2: FF, FB and hybrid controller attenuation in the case of a pure
              tone at $\Omega = 105$ Hz
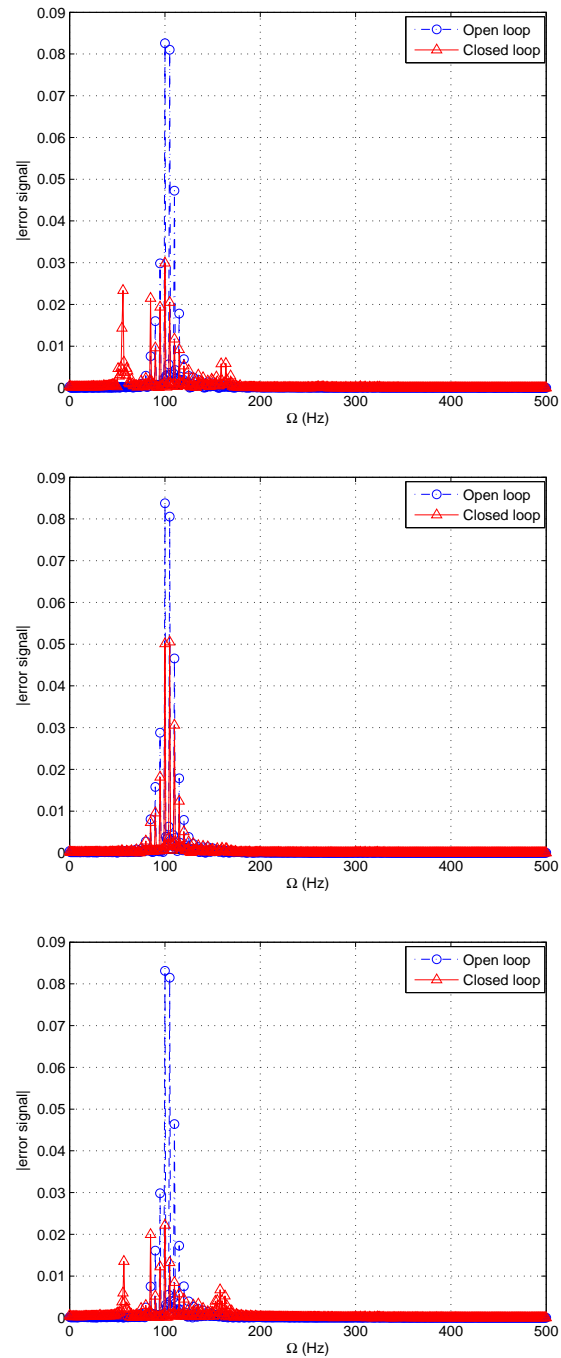
Figure 6.3: FF, FB and hybrid controller attenuation in the case of the
                 synthetic fan $\Omega \in [95, 115]$ Hz
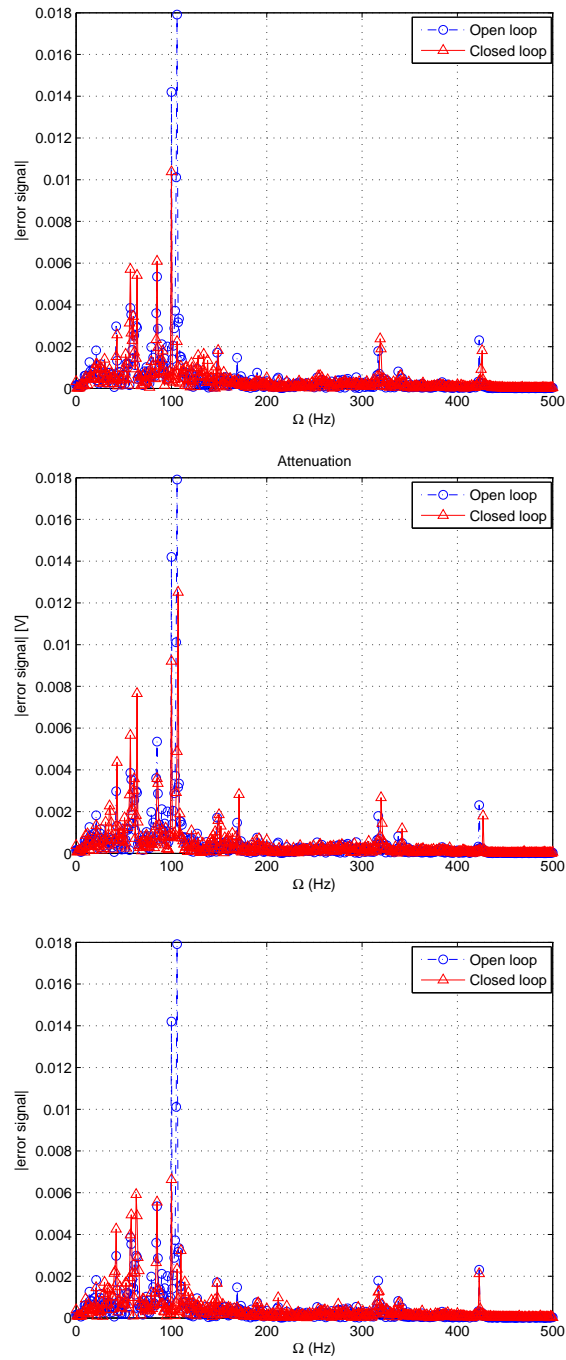
Figure 6.4:   FF, FB and hybrid controller attenuation in the case of the
             industrial fan
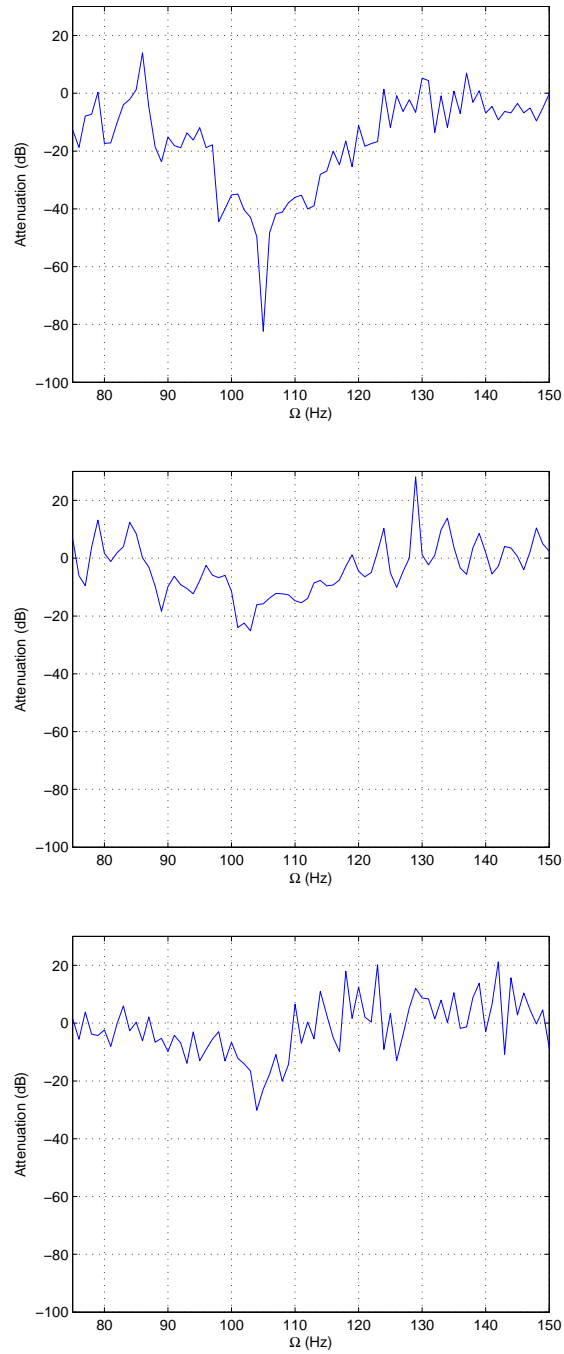
Figure 6.5: Hybrid controller attenuation with the three different input
signals
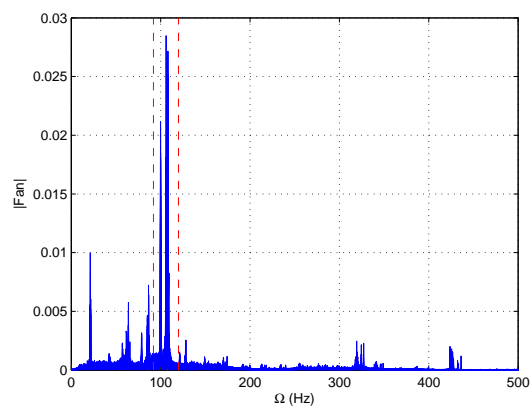
Figure 6.6: Output of the primary path excited by the fan and ideal
             performance region (inside the dashed lines)

CHAPTER 7

SENSOR/ACTUATOR ALLOCATION

As a consequence of all comments stated in Section 2.3, this part of the work is focused in computing a practical measure for S/A allocation, previous to controller design and implementation[1]. The general control configuration in Figure 2.2 will be used, based on Linear Fractional Transformations (LFT), which accommodate many practical applications. The basic characteristics of these type of applications are: a stable uncertain plant with time delays and/or RHP zeros, lightly damped dynamics and, as with many other applications with *fast* dynamics, the need of a low order controller for real time implementation. The measure sought combines relevant issues concerning performance, robustness and implementation. The approach presented here is focused in computing the optimal S/A combination achieving the best performance and controller complexity, assuming that a controller exists which can be easily verified in general, *e.g.* for mixed sensitivity $\mathcal{H}_\infty$ control use condition in [DGKF89]. The performance weight $W_p(s)$ and its corresponding bandwidth Ω where noise attenuation is desired is also a problem input data.

A part of the S/A location measure considers properties of the model itself as its *numerical* order, computed by means of the Hankel Singular Values (HSV). Hence it includes simultaneously W_c and W_o, and therefore takes into account the controller order (proportional to the augmented model order), a key issue for real time implementation. Model uncertainty is considered as global and dynamic, which provides a fairly general way to describe many practical

---

[1]Here, equivalent conditions are computed for $\mathcal{H}_\infty$ optimal controller existence, previous to building, implementing or testing the actual controller. Controller existence can be verified using the three conditions based on the performance measure γ [DGKF89]. Alternative options in the one and four block problems are also provided [SS98].

situations without excessive conservativeness. Instead, structured dynamic or parametric uncertainty may lead to higher order and/or suboptimal controllers, as in the case of μ–synthesis or non-optimal parametric design procedures. In addition, works focused on performance under structured uncertainty models [LBMP94] cannot compute an S/A measure previous to controller design.

Furthermore, the bandwidth and performance limitations imposed by model uncertainty and nonminimum phase zeros are also taken into account, the latter based on [FHMT03] for the general setup in Figure 2.2. Hence, the performance and uncertainty weights are problem input data. The computation of all the measures can be made with standard software either for SISO or MIMO models. Without loss of generality stable systems are considered, which still cover many important applications, *e.g.* vibration and acoustics active control, robotics, large space structures, etc. Similar tools as the ones presented in this work can be generated in the case of unstable systems[2]. With the same approach, some preliminary results have been presented by the authors in [SPCiE08], and tested on duct simulations based on the model in Section 3.2 [HAV$^+$96]. Here instead, an update of the S/A measures and a full experimental testing of the methodology has been made.

Finally, as mentioned in [JT98] it is unlikely that the methods that solve the S/A selection problem have polynomial time complexity, since most of the methods are indirect in the sense that a candidate-by-candidate test should be performed. Nevertheless controller design and implementation are not necessary in order to compute the S/A location measure in this case (see footnote 1), which reduces the time search. Therefore, based on the evaluation characteristics of S/A location methods, the one presented here is: well-founded, efficient (because it does not involve controller implementation, although it is not polynomial-time complexity), generally applicable (it uses the general structure in Figure 2.2), rigorous (it considers performance, robustness and implementation), quantitative, controller independent and indirect.

The chapter is organized as follows: In next section some background material and the control design setup are presented. In section 7.2 the main results of this chapter are introduced. Finally, the real example presented in Chapter 3 illustrates the application of these measures in an acoustic tube used for active noise control (ANC) and is validated against experimental data in section 7.3.

---

[2]For example, the limitations due to unstable poles can also be obtained from [FHMT03], the computation of the HSV can be separated among stable and unstable subsystems, and care must be taken when considering the set of uncertain models that all have the same number of unstable poles, when describing them as global dynamic uncertainty.

7.1   Background and Control Problem Motivation

The control configuration adopted is the general one in Figure 2.2, which represents all possible linear control problems. Here $G(s)$ is the augmented model which includes not only the nominal plant $G_{yu}(s)$ but also the specification weights, *e.g.* performance, uncertainty, actuator bounds, etc.

$$G(s) \;\; = \;\; \begin{bmatrix} G_{zw}(s) & G_{zu}(s) \\ G_{yw}(s) & G_{yu}(s) \end{bmatrix}, \qquad T_{zw} = F_\ell\left[G(s), K(s)\right]$$

Also w is the disturbance vector, z the vector of signals to be minimized, (u, y) the input and outputs of the system, and $F_\ell\left(\cdot\right)$ the lower linear fractional transformation operator. This setting may consider general performance and robustness constraints and applies not only to SISO but also to MIMO systems. For example, the performance objective may be represented by the weight $W_p(s)$ on the error signal, which has larger values in the bandwidth Ω where attenuation is desired. Without loss of generality, robust performance quantified by $\|T_{zw}(s)\|_\infty$ could represent a typical mixed sensitivity problem. Another way of representing the same problem would be $\|T_{zw}(s, \gamma)\|_\infty < 1$, where the minimum γ that weights performance, *e.g.* $\frac{1}{\gamma}W_p(s)$, is sought.

7.1.1   Model realizations

S/A allocation is an important part of the identification and control problem in most applications. Nominal model-based measures [LAKB01], or even uncertain model-based criteria [PP06] which evaluate S/A allocation, are based on the controllability and observability grammians W_c and W_o. These measures depend on the state definition and furthermore, sensor and actuator location problems are treated independently, based on both grammians separately. Here instead, measures that involve the system as a whole from an input/output perspective, are needed.

   To avoid this, in this work a standard state-space representation of models is used, which has been extensively employed for model order reduction [Moo81, Glo84]. This is the internally balanced state-space realization which has the particular advantage that both grammians are

equal and diagonal, with the (ordered) Hankel singular values in their diagonal, *i.e.*

$$
W_c = W_o = \begin{bmatrix} \sigma_1^H & \cdots & 0 \\ \vdots & \ddots & \vdots \\ 0 & \cdots & \sigma_n^H \end{bmatrix}
$$

It provides the optimal balance between controllability and observability and allows a stable and balanced model order reduction by truncation of the states corresponding to the smallest Hankel singular values. In addition, a bound on the reduction error can be obtained as a function of these values. More importantly, balanced realizations provide the minimal condition number of the observability and controllability grammians [Moo81] over all possible state space realizations, *i.e.*

$$
\min_T \max \left[\kappa(W_o), \kappa(W_c) \right] = \frac{\sigma_1^H}{\sigma_n^H}
$$

where $\kappa(W) = \frac{\bar{\sigma}(W)}{\underline{\sigma}(W)}$ is the condition number. This allows a coherent distribution of the states, so that the "more" (higher Hankel singular values) controllable ones are also the "more" observable ones.

As in any practical case, if accessibility is guaranteed (the states accessible from the inputs, and the outputs from the states) necessary and sufficient conditions for structural state controllability and observability are guaranteed according to [MS80].

7.1.2   Performance limitations

Concerning performance limitations, a recent work has been made for the feedback structure adopted here (Figure 2.2) and in [FHMT03], which generalizes the one in [FL85]. The limitations imposed by RHP poles and zeros have been quantified and they reduce to the usual limitations for a standard feedback loop [FL85] when $\det[G] \equiv 0$ and then the LFT is said to be *reducible* to a feedback loop. This is the case when the performance output is measured for feedback $z = y$ or when the control and disturbance excite the system in the same point, $w = u$. As commented previously, without loss of generality the RHP pole limitations will not be considered here.

In the general case ($\det[G] \neq 0$), the algebraic limitations on robust performance $\|T_{zw}\|_\infty$ are imposed by the RHP zeros $(\varsigma_1, \ldots, \varsigma_m)$ of G_{zu} or G_{yw} with multiplicities satisfying

$m_{zw}(\varsigma) < m_{zu}(\varsigma) + m_{yw}(\varsigma)$ and are quantified as follows:

$$\begin{aligned} \|T_{zw}\|_\infty &\geq \max_j |G_{zw}^o(\varsigma_j)| \overset{\triangle}{=} \gamma_z \\ G_{zw}(s) &= G_{zw}^o(s)B_\varsigma(s) \end{aligned} \tag{7.1}$$

where $B_\varsigma(s)$ is the Blaschke product corresponding to all RHP zeros ς_j, which absorbs them from $G_{zw}(s)$ (Corollary IV.2 of [FHMT03]). As a consequence, γ_z poses a lower limit to the robust performance measure γ. Usually the RHP zeros of the model G_{yu} constraint the sensitivity function, but note here that they only contribute to the performance limitation in the case reducible to a feedback loop, *i.e.* $\det(G) = 0$.

Measure γ_z quantifies the RHP zeros limitation but is just a lower bound on the closed loop transfer function performance and may not be representative of the actual performance of the loop when $\gamma \gg \gamma_z$. Thus, a more realistic value of the optimal performance could be considered in order not to provide exceedingly conservative results.

7.1.3 Robust performance computation

To this end, the exact value of γ can be computed beforehand based on the Youla parametrization approach in order to solve the $\mathcal{H}_\infty$ problem, see [CDL86, Doy84]. All possible closed loop models can be represented as:

$$T_{zw} = T_{11} + T_{12}QT_{21}, \qquad Q \in \mathcal{H}_\infty \tag{7.2}$$

assuming the loop is well posed. Since the $\mathcal{H}_\infty$ norm is invariant under multiplication by unitary matrices, the problem can be transformed into:

$$\begin{aligned} \|T_{zw}\|_\infty &= \|T_{11} + T_{12}QT_{21}\|_\infty \tag{7.3} \\ &= \left\| \begin{bmatrix} T_{12,\perp} & T_{12} \end{bmatrix}^\sim (T_{11} + T_{12}QT_{21}) \begin{bmatrix} T_{21,\perp} \\ T_{21} \end{bmatrix}^\sim \right\|_\infty \tag{7.4} \\ &= \left\| \begin{bmatrix} R_{11} & R_{12} \\ R_{21} & R_{22} + Q \end{bmatrix} \right\|_\infty \tag{7.5} \end{aligned}$$

where

$$R \triangleq \begin{bmatrix} R_{11} & R_{12} \\ R_{21} & R_{22} \end{bmatrix} = \begin{bmatrix} T_{12,\perp} & T_{12} \end{bmatrix}^{\sim} T_{11} \begin{bmatrix} T_{21,\perp} \\ T_{21} \end{bmatrix}^{\sim} \tag{7.6}$$

Here R is completely anti-stable and can be built from the augmented model $G(s)$ which includes the specification weights as well as the nominal model, $T_{\perp}$ is the orthogonal complement and $A^{\sim}(s) = A^T(-s)$ the adjoint operator. The $\mathcal{H}_{\infty}$ controller synthesis can be recast as the following approximation problem:

$$\gamma = \inf_{Q_a} \left\{ \|R + Q_a\|_{\infty} : Q_a = \begin{bmatrix} 0 & 0 \\ 0 & Q \end{bmatrix}, Q \in \mathcal{H}_{\infty} \right\} \tag{7.7}$$

This is called the four-block problem and can be solved exactly before building the controller in two cases.

- In the one block problem, *e.g.* optimal nominal performance, Equation (7.7) can be solved as a Nehari approximation problem

$$\gamma = \inf_{Q} \left\{ \|R + Q\|_{\infty} \, Q \in \mathcal{H}_{\infty} \right\} = \|\Gamma_R\| = \|R\|_H$$

where $\|\Gamma_R\|$ is the Hankel operator for R and $\| \cdot \|_H$ its Hankel norm.

- Using the all-pass embedding [Par78] and based on the procedures in [GLD$^+$91] and [LKJS88], the equivalence between the one- and four-block problems can be proved (see also [SS98]). Hence, from Equation (7.7) the optimal γ can be computed exactly by solving a pair of Ricatti equations and a spectral radius condition, when the following restriction applies:

$$\gamma > \max \left\{ \left\| \begin{bmatrix} R_{11} & R_{12} \end{bmatrix} \right\|_{\infty}, \left\| \begin{bmatrix} R_{11} \\ R_{21} \end{bmatrix} \right\|_{\infty} \right\}$$

In general and similar to the previous result, the exact value of γ can be obtained from the $\mathcal{H}_\infty$ solution proposed in [DGKF89], also known as the DGKF approach. Here $\|T_{zw}\|_\infty < \gamma$ if and only if the following conditions are achieved:

i) $H_\infty \in dom(Ric)$ and $X_\infty \triangleq Ric(H_\infty) \geq 0$

ii) $J_\infty \in dom(Ric)$ and $Y_\infty \triangleq Ric(J_\infty) \geq 0$

iii) $\rho(X_\infty Y_\infty) < \gamma^2$

where H_∞ and J_∞ stand for two Hamiltonian matrices:

$$H_\infty \triangleq \begin{bmatrix} A & \gamma^{-2}B_1 B_1^T - B_2 B_2^T \\ -C_1^T C_1 & -A^T \end{bmatrix}, \quad J_\infty \triangleq \begin{bmatrix} A^T & \gamma^{-2}C_1^T C_1 - C_2^T C_2 \\ -B_1 B_1^T & -A \end{bmatrix}$$

Here the Hamiltonian domain is represented by $dom(Ric)$, which meets all necessary conditions to have a unique solution of the Ricatti equation, $\rho(\cdot)$ is the spectral radius and the open loop data of the augmented plant is:

$$G \equiv \left[\begin{array}{c|cc} A & B_1 & B_2 \\ \hline C_1 & 0 & D_{12} \\ C_2 & D_{21} & 0 \end{array} \right]$$

Here γ is computed by means of the equivalent conditions i) to iii), but building the controller is not actually needed. It may be argued that building the controller is just at a short step from this point, but more importantly, controller implementation and test are not needed neither, and here is where most of the work for the S/A selection is usually done.

Next two bounds for γ which will be used in the sequel, are defined. For RP, the optimal solution to the worst case model/disturbance problem $\|T_{zw}\|_\infty$ is represented as $\overline{\gamma}$, *e.g.* in a mixed sensitivity problem:

$$\left\| \begin{array}{c} S(s)W_p(s) \\ T(s)W_\delta(s) \end{array} \right\|_\infty \leq \overline{\gamma} \tag{7.8}$$

On the other hand, NP is defined as the worst case performance for the *nominal* model, the optimal being $\underline{\gamma}$. For example, in a tracking error minimization under energy bounded output weighted by $W_p(s)$ disturbances problem, it stands as follows:

$$NP \iff \|S(s)W_p(s)\|_\infty \leq \underline{\gamma} \tag{7.9}$$

Here $\underline{\gamma}$ can be computed as $\|R\|_H$, due to the fact it is a one-block problem. As a consequence, the actual plant will have a performance level γ bounded by

$$0 < \gamma_z \leq \underline{\gamma} \leq \gamma \leq \overline{\gamma} \tag{7.10}$$

7.1.4 Model uncertainty

There are many model uncertainty representations, dynamic, parametric, structured, unstructured. One of the most used in practice is global dynamic multiplicative uncertainty [DFT92]:

$$\mathcal{G} \triangleq \left\{ \tilde{G} = [I + \Delta W_\delta(s)]\, G_o(s),\ \bar{\sigma}\,[\Delta] < 1 \right\} \tag{7.11}$$

This is due to the fact that it accommodates many practical cases which include: high order unknown dynamics, linearization uncertainty, infinite dimensional models, unknown time delays all of which apply to mechanics, aerospace, acoustics and many other engineering problems. In addition, in a simple RS problem with this type of uncertainty and a typical high-pass uncertainty weight $W_\delta(s)$, its crossover frequency poses an upper limit for the performance bandwidth or, in other words, performance can be achieved at those frequencies where $\bar{\sigma}\,[W_\delta(\jmath\omega)] < 1$ because:

$$RS \iff \bar{\sigma}\,[W_\delta(\jmath\omega)T(\jmath\omega)] < 1 \quad \forall\omega \tag{7.12}$$

$$\bar{\sigma}\,[W_\delta(\jmath\omega)] \geq e_{rel}(\jmath\omega) = \bar{\sigma}\left\{\left[\tilde{G}(\jmath\omega) - G_o(\jmath\omega)\right]G_o^{-1}(\jmath\omega)\right\} \in \mathbb{R} \tag{7.13}$$

As a consequence, the limitations on the **performance bandwidth** due to model uncertainty can be quantified as follows:

$$\Omega_p = \left\{ \begin{array}{l} \sum_{i=1}^n (\omega_i^u - \omega_i^\ell),\ \forall\omega \in [\omega_1^\ell, \omega_n^u] \subseteq \Omega \text{ such that} \\ e_{rel}(j\omega) \leq 1 \end{array} \right\} \tag{7.14}$$

where clearly $\omega_i^u \geq \omega_i^\ell$, $\forall i = 1, \cdots, n$. This measures the relative size of the bandwidth with

respect to the desired one (Ω) for which robust performance should be achieved. It may well be zero if such conditions are not met, *i.e.* the relative error $e_{rel}(\jmath\omega) > 1$ in Equation (7.13) for all frequencies ω, hence robust performance cannot be achieved in that case.

On the other hand, the direct limitation on RP due to the size of the uncertainty could be measured by means of a different parameter. Again, taking the example of the mixed sensitivity problem described previously, a sufficient condition for robust performance is:

$$RP \quad \Longleftarrow \quad \bar{\sigma}\left[W_p(s)S(s)\right] + \bar{\sigma}\left[W_\delta(s)T(s)\right] < 1 \tag{7.15}$$

Then the relative error size may be directly considered to measure performance limitations as follows:

$$\ell_{e_{rel}} \quad = \quad \min\left\{1, \left(\max_{\omega\in\Omega} e_{rel}(\jmath\omega)\right)\right\} \tag{7.16}$$

Here the fact that W_δ is defined by Equation (7.13) is used. Another index could compare W_δ with the actual relative error e_{rel} to indicate if the uncertainty weight has been chosen correctly, as will be seen in next section.

Furthermore, some bounds on (7.15) can be stated [Glo84]:

$$\bar{\gamma} \quad \leq \quad \bar{\sigma}\left[W_p(s)S(s)\right] + \bar{\sigma}\left[W_\delta(s)T(s)\right] \leq 2\bar{\gamma} \tag{7.17}$$

$$RP \quad \Longleftarrow \quad 2\bar{\gamma} < 1 \tag{7.18}$$

7.1.5 I/O relative gains

Another important issue in control problems is the I/O relative gains of the system to be controlled, which may be represented by its condition number $\kappa\left[G(s)\right]$. It plays an important role in many practical situations, *e.g.* high-purity distillation, see [SMD88], as a factor in the interplay between performance and input dynamic uncertainty, clearly only for MIMO systems. For example in a classical loop-shaping design where the tracking error attenuation is weighted by $W_p(s)$, a sufficient condition for robust performance is affected by this parameter when global **input** actuator dynamic uncertainty weighted by $W_\delta(s)$ is present [ZDG96, SS98], *i.e.*

$$RP \quad \Longleftarrow \quad \kappa\left[G(s)\right]\bar{\sigma}\left[W_p(s)S(s)\right] + \bar{\sigma}\left[W_\delta(s)T(s)\right] < 1, \quad \forall s = \jmath\omega \tag{7.19}$$

As a consequence, RP decreases at frequencies where $\kappa\left[G(\jmath\omega)\right]$ is large.

7.1.6   Recap

As a result of all the above considerations, several quantifiable values can be related with performance, robustness and controller implementation:

- Right half–plane zeros limit performance in the general case $(\det[G] \neq 0)$ as indicated in Equation (7.1). A usual interpretation [DFT92] considers that they pose a similar performance limitation as dynamic uncertainty.

- Model errors quantified as global multiplicative dynamic uncertainty, pose a robust performance bandwidth limitation measured by Ω_p in (7.14) and also quantified by $\ell_{e_{rel}}$ in (7.16).

- The controller order is directly related to the *numerically sensible* model order. The latter is obtained from the set of positive Hankel singular values of the system's model balanced realization.

- In the case of MIMO systems, the nominal model condition number $\kappa(G_o)$ combined with actuator (input) dynamic uncertainty is also a performance limiting factor.

In the main part of this work which will be presented in next section, the criteria to define the S/A optimal location takes into account the final goal pursued by any identification and control methodology: closed loop robust performance and controller implementation. Hence, all these items will be taken into consideration when defining measures that quantify the S/A allocation. Furthermore, these S/A measures may be computed *before* the actual controller is designed and/or tested, in order to minimize the combinatorial search over all S/A locations.

7.2   S/A Allocation Measure

Several S/A location measures will be defined in a normalized way as follows:

- Their values are between 0 and 1.

- Higher values represent better situations from the performance and controller implementation standpoint, *e.g.* lower controller order and higher performance increase the values of the corresponding measures.

- All the measures must be calculated before building or implementing the controller, based only on the identified model, its corresponding uncertainty and the specification weights.

In addition, and in order to have good numerical properties of the plant's model for controller design, an internally balanced realization of the nominal model at each S/A location is defined as $G_i(s) = G_{yu}(s)$, $i = 1, \cdots, N$. Here each pair of S/A location is represented by an integer i, with $i = 1, \cdots, N$. Set $\mathcal{S}$ represents a selected group of these S/A locations pairs.

To consider performance measures, the following values are defined.

$$\underline{\gamma}_{\min} = \left\{ \min_i \underline{\gamma}_i, \quad i = 1, \cdots, N \right\} \tag{7.20}$$

$$\overline{\gamma}_{\min} = \left\{ \min_i \overline{\gamma}_i, \quad i = 1, \cdots, N \right\} \tag{7.21}$$

where $\underline{\gamma}$ and $\overline{\gamma}$ have been defined in section 7.1.3.

Next, the partial measures which quantify robustness, performance and controller implementation are defined for the i–th S/A location.

Definition 7.1. The influence of the controller order is quantified as follows:

$$\rho_o(i) \triangleq \left\{ n + 1 \mid \min_n \sigma_n^H [G_i(s)] > \epsilon_r \right\}^{-1} \tag{7.22}$$

Here σ_n^H are the Hankel singular values, $G_i(s)$ is the augmented model at the i–th S/A location, and $\epsilon_r > 0$ is a predefined (controllability/observability) safety margin[3]. The $(n + 1)$ term takes into consideration the possibility of a constant model, *i.e.* order $n = 0$, otherwise only n should be considered in the definition.

Definition 7.2. The following defines a deterministic performance S/A location measure.

$$\rho_{p_d}(i) \triangleq \begin{cases} 0 & \text{if} \quad 2\overline{\gamma}_{\min} \leq \underline{\gamma}_i \\ 1 & \text{if} \quad 2\overline{\gamma}_{\min} > \underline{\gamma}_i \end{cases} \quad , \quad i = 1, \cdots, N \tag{7.23}$$

---

[3]Recall that $\sigma_n^H = 0$ or *numerically* near to zero implies an uncontrollable and/or unobservable state space representation. Another alternative is to use the subspace identification criteria [OM94, Ver94] to select the model order.

The idea behind this measure follows from Equations (7.10) and (7.17). Here, the S/A pairs that achieve $\rho_{p_d}(i) = 0$ will have their full range of performances worse than other pairs, *i.e.* their best performance $\underline{\gamma}_i$ is always higher than the worst performance bound $2\overline{\gamma}_{\min}$ of other pairs, hence these locations could be excluded. To illustrate this, consider an example of four different S/A pairs, as depicted in Figure 7.1:
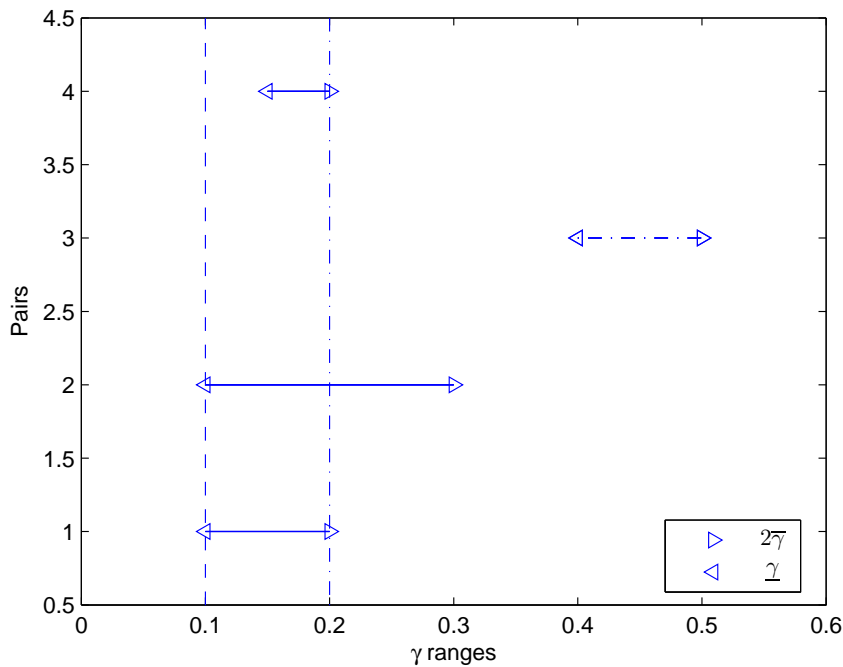
Figure 7.1: γ range selection case example.

Example 3. Using the criteria given in (7.23), $2\overline{\gamma}_{\min} = 0.2$ (dashdot line in Figure 7.1) so $2\overline{\gamma}_{\min} \le \underline{\gamma}_3$. Thus, the dashdot pair $i = 3$ is excluded, hence the selected set is $\mathcal{S} = \{1, 2, 4\}$.

In the previous example, there are still three pairs which cannot be deterministically excluded. Hence, a criteria which complements the previous one should be defined to select among the remaining pairs. This should consider other characteristics of the performance intervals at each S/A location.

Definition 7.3. To measure how uncertainty could potentially limit robust performance the following is defined.

$$\rho_{\delta_{error}}(i) \quad \triangleq \quad 1 - \ell_{e_{rel}}(i), \quad i = 1, \cdots, N \tag{7.24}$$

Here $\ell_{e_{rel}}$ is defined in (7.16) and $\rho_{\delta_{error}}$ is therefore related to Equations (7.13) and (7.15). Note that robust performance is only possible when $\ell_{e_{rel}} < 1$ and $W_\delta(s)$ has been selected conveniently. Hence, $\rho_{\delta_{error}}$ measures how severely model uncertainty of a certain S/A location limits performance. This measure could well be combined or merged with the previous one, due to the fact that both produce similar effects over robust performance.

Since all the S/A selection measures presented in this section depend on the nominal model $G_o(s)$, high values of $\rho_{\delta_{error}}$ are needed in order to make the other measures reliable. In addition, when $\rho_{\delta_{error}}$ is very low, it may also be used *a posteriori* in order to decide whether a better identification could produce a higher performance at certain S/A locations.

Definition 7.4. Uncertainty can also limit the bandwidth where performance should be achieved, and can be measured as follows.

$$\rho_\Omega(i) \quad \triangleq \quad \frac{\Omega_p}{|\Omega|}, \quad i = 1, \cdots, N \tag{7.25}$$

Here Ω_p is defined in (7.14) with the nominal model $G_o(s)$ replaced by $G_i(s)$ where $|\Omega|$ is the size of the desired performance bandwidth.

Definition 7.5. A measure which defines how adequately has the uncertainty weight been selected, *i.e.* the match between the relative model error e_{rel} and the W_δ, can be defined as follows.

$$\rho_m \quad \triangleq \quad 1 - \min\left\{ 1, \max_{\omega \in \Omega} \bar{\sigma}\left[W_\delta(j\omega) - e_{rel}(j\omega)\right] \right\} \tag{7.26}$$

A pathological case would be when $\rho_m = 0$, that is, when the extra uncertainty added by a bad fit between W_δ and the error equals 100%. Here, even if the best possible model could be identified, *i.e.* $\rho_{\delta_{error}} = 1$, no performance could be achieved. As well as $\rho_{\delta_{error}}$, ρ_m is also an important measure, because it modifies the value of $\overline{\gamma}_i$ in (7.8) and hence of ρ_{p_d} in (7.23). Here again, high values of ρ_m should be also sought in order to make ρ_{p_d} trustable. Note also that low values of ρ_m just add conservativeness, but on the other hand it may also be used

a posteriori in order to decide whether a better uncertainty weight selection could produce a higher performance at certain S/A locations.

Definition 7.6. To measure the potential performance that can be obtained in each S/A pair, the following is defined:

$$\rho_{\gamma_{\min}}(i) \;\; \triangleq \;\; \frac{\underline{\gamma}_{\min}}{\underline{\gamma}_i}, \quad i = 1, \cdots, N \tag{7.27}$$

The closer $\rho_{\gamma_{\min}}$ is to 1 (accordingly $\underline{\gamma}_{\min}$ closer to $\underline{\gamma}_i$), the (potentially) better the performance of pair i might be as compared to all the remaining S/A pairs. Considering again example 3 (Figure 7.1), it can be seen how the remaining pairs are arranged according to (7.27). The locations $i = 1$ and $i = 2$ are the best, because they both have the lowest $\underline{\gamma}_i$ and $i = 4$ is the worst because it has the largest $\underline{\gamma}_i$. Pair i=3 has already been discarded by ρ_{p_d}.

Alternatively, γ_{z_i} may be used instead of $\underline{\gamma}_i$ to calculate this measure. Consequently, $\underline{\gamma}_{\min}$ in (7.20) is redefined as $\underline{\gamma}_{\min} = \left\{ \min_i \gamma_{z_i}, \quad i = 1, \cdots, N \right\}$ and also $\rho_{\gamma_{\min}}(i) \triangleq \underline{\gamma}_{\min}/\gamma_{z_i}$. This would lead to more conservative results, but computation of $\underline{\gamma}_i$ would be omitted for all pairs.

Definition 7.7. The measure which relates robust performance with the limitation imposed by the model condition number, useful only for MIMO systems with actuator uncertainty, is defined as follows:

$$\rho_{\kappa}(i) \;\; \triangleq \;\; \left\{ \frac{\max_\omega \bar{\sigma}\left[W_p(\jmath\omega)\right] \kappa\left[G_i(\jmath\omega)\right]}{\max_\omega \bar{\sigma}\left[W_p(\jmath\omega)\right]} \right\}^{-1} \quad i = 1, \cdots, N \tag{7.28}$$

All these measures contribute to determine an optimal value for the S/A location, although they quantify different aspects of robust performance and implementation issues. Measures ρ_κ and $\rho_{\delta_{error}}$ are amenable to be combined due to the fact that they are related to the same Equation (7.19). In any case, the user could take all these issues into consideration by defining a general weighted combination of all previous values as follows:

Definition 7.8. A general control-oriented S/A measure can be defined as a convex combination of all the previous ones:

$$\rho_{as}(i) \;\; = \;\; \sum_{\ell \in \mathcal{S}} w_\ell \, \rho_\ell(i), \quad i = 1, \cdots, N, \quad \mathcal{S} = \{o, m, p_d, \kappa, \delta_{error}, \Omega, \gamma_{min}\}$$

The weights $w_\ell \in [0, 1]$ with $\sum_{\ell \in \mathcal{S}} w_\ell = 1$.

The previous are constant real values which weight the relative importance of performance and controller implementation, and are supplied by the user. The weight $w_\kappa = 0$ in cases where the system is SISO or when sensor instead of actuator uncertainty dominates the global dynamic model set as in $\mathcal{G}$ in Equation (7.11). This measure will therefore be normalized in the interval $[0, 1]$. Here the problem is how to select the weights according to practical considerations.

Another alternative is to select a set $\mathcal{S}$ with the best S/A locations according to each measure and intersect them in order to make a pre-selection. In cases where the measures quantify different aspects of the problem, *e.g.* ρ_o and ρ_Ω, there is the possibility that best S/A selection of each will not coincide, *i.e.* their intersection is empty. In these cases, one may give more importance to one aspect over the other and relax the sets until there is intersection between them. Instead, if the measures quantify a similar aspect like the uncertainty measured by ρ_Ω and $\rho_{\delta_{error}}$, it is more likely that their intersection exists. This approach will be attempted in the example presented in next section.

7.2.1 Dependencies between measures

Some hierarchy between S/A measures can be posed, which is summarized in Table 7.2.1.

Measure	$\rho_{\delta_{error}}$ **(critical)**	ρ_m **(conservative)**
ρ_{p_d}	dependent	dependent
$\rho_{\gamma_{\min}}$	dependent	independent
ρ_Ω	dependent	independent
ρ_κ	dependent	independent
ρ_o	dependent	independent

Table 7.1: S/A measure dependencies

Dependencies on $\rho_{\delta_{error}}$ are critical, since it measures the quality of the identified nominal model G_o within Ω, and thus the reliability of the results derived from the use of this model. A bad model identification compromises the trust on $\overline{\gamma}_i$ and $\underline{\gamma}_i$ ((7.8) and (7.9)) because it is not known how this model mismatch will affect the γ measures which could increase or decrease indistinctly. Other measures depending on $\underline{\gamma}_i$ and $\overline{\gamma}_i$ will be similarly affected and hence non-reliable conclusions could be derived from them, *e.g.* set of pairs discarded. As shown in Table 7.2.1, all measures depend on $\rho_{\delta_{error}}$ therefore good model identification is compulsory

in order to obtain a trustworthy selection methodology.

On the other hand, dependencies on ρ_m are not critical because only reliability on $\overline{\gamma}_i$ is compromised, *i.e.* $\underline{\gamma}_i$ remains the same if ρ_m is changed, because it doesn't depend on the uncertainty model, as shown in (7.9). Note that low values of ρ_m always increase $\overline{\gamma}_i$, which means that more uncertainty only adds conservativeness to the results, *e.g.* less discarded pairs than would potentially be expected with higher values of ρ_m. Also note that this can be fixed *a posteriori* if desired, without decreasing the set of discarded pairs, in the sense that better values of ρ_m can be reached without modifying G_o but only W_δ. Instead an *a posteriori* fix of $\rho_{\delta_{error}}$ implies a further identification of the system. As a consequence, ρ_m can be modified without changing $\underline{\gamma}_i$, which means that improving ρ_m is always potentially good in order to make the decision criteria better, *i.e.* discarding more pairs. This procedure will be illustrated in the example presented next.

7.3 Experimental Example

A real application presented in Chapter 3 illustrates the usefulness of the S/A allocation measures derived previously. The proposed active-noise control scheme uses a feedback configuration that requires only one sensor, the error microphone illustrated in the conceptual setup in Figure 3.4(a). With this scheme, some preliminary results have been presented by the authors in [SPCiE08], and tested on duct simulations based on a model in [HAV+96]. Here instead, an update of the S/A measures and a full experimental testing of the methodology has been made.

7.3.1 Results

Some *a priori* specifications and information from the experimental plant have been taken into account before deciding the grid considered, in order to make the best sensor/actuator location selection. In this example, a grid of two sensor by four actuator positions in the duct (Figure 3.1) have been considered to evaluate eight different S/A location pairs.

The measures introduced in the previous section will be used to decide the best locations, based on performance and implementation issues, before the controller design and implementation. Here in addition, the methodology is validated *a posteriori* by designing controllers for all test locations and computing their performance and order. The performance of each controller

within Ω is measured as follows.

Definition 7.9. Weighted attenuation λ, used to measure the performance weighted by W_p, is defined as follows:

$$\lambda(i) \triangleq \frac{\|W_p(s)y_{i_*}\|_2}{\|w_{i_*}\|_2} \leq \sup_{\omega \neq 0} \frac{\|W_p(s)y\|_2}{\|\omega\|_2} = \|W_p \cdot S_{\Delta_*}\|_\infty, \quad i = 1, \cdots, N \qquad (7.29)$$

where y_{i_*} and w_{i_*} stand for real output and real exogenous perturbation, respectively.

In order to compare robust performance with the previous bounds, note that:

$$RP \iff \gamma_{RP} \quad \triangleq \quad \sup_{\Delta \in \boldsymbol{\Delta}} \|W_p(s)S_\Delta(s)\|_\infty < 1 \qquad (7.30)$$

$$S_\Delta \quad \triangleq \quad \{I + [I + \Delta W_\delta(s)]\, G_o(s)K(s)\}^{-1}, \bar{\sigma}\,(\Delta) < 1 \qquad (7.31)$$

where S_Δ is the uncertain sensitivity function and $K(s)$ is the implemented controller. There-fore according to Equations (7.10), (7.17) and (7.29), γ_{RP} is bounded as follows:

$$0 < \gamma_z \leq \underline{\gamma} \leq \lambda \leq \|W_p \cdot S_{\Delta_*}\|_\infty \leq \gamma_{RP} \leq 2\overline{\gamma} \qquad (7.32)$$

These bounds will be used to validate the experimental results, as illustrated in Figure 7.2. The best locations selected by the measures should at least *include* the ones produced by the actual controllers.

The general selection procedure is summarized as follows:

1. Check S/A measures reliability

    1.1 Compute $\rho_{\delta_{error}}$

    1.2 Compute ρ_m to measure conservativeness

2. Compute ρ_o to measure controller implementation

3. Compute potential performance of S/A pairs

    3.1 Check RP bound on (7.18) for S/A pair containing $\overline{\gamma}_{\min}$

    3.2 Filter pairs using ρ_{p_d} measure

4. Post-filter S/A pairs by other measures

    4.1 Discard non-deciding intervals

    4.2 Obtain optimal set $\mathcal{S}_m$ of S/A pairs for each measure

5. Intersection of previous sets to select the optimal one: $\cap_m \mathcal{S}_m = \mathcal{S}_{opt}$. If necessary, the selection should be increased until the intersection makes sense.

6. Check Robust Performance before controller implementation, if (7.18) does not hold for the pair selected, check *a posteriori* RP with (7.30)

Finally, as commented in definition 7.5 and section 7.2.1, ρ_m can be used as an *a posteriori* measure to increase performance, at the expense of changing the S/A selection. This is performed by searching for the pair that has the worst fit between model uncertainty and W_δ, *i.e.* lower ρ_m, and the best potential performance, *i.e.* higher $\rho_{\gamma min}$. The argument is clear: reconsider S/A pairs which have good chances to increase performance (high $\rho_{\gamma min}$) due to the fact that a poor selection of W_δ has been made in these cases (low ρ_m). The S/A pair selection is made by intersecting both sets as in the main selection procedure. The selection procedure and an *a posteriori* change in the final selection are applied to the example in the following paragraphs.

First, $\rho_{\delta_{error}}$ is computed in order to verify the reliability of all measures which depend on the nominal model G_o. Here, the lowest value of $\rho_{\delta_{error}}$ is 0.9753 (pair $i = 8$), which means that the worst fit between model error and data within Ω for all pairs is below 3%, a reasonably good fit.

Secondly, ρ_m is computed and for pair $i = 8$, $\rho_m = 0.5573$, hence the selection of W_δ adds an extra 44.27% of uncertainty to the nominal model G_o and as a consequence more conservative results. This could be mended *a posteriori* without affecting the *a priori* S/A selection, just by improving the fit between W_δ and the relative uncertainty error e_{rel}. Anyhow, improving ρ_m means obtaining at least the same number of pairs discarded than before. This cannot be guaranteed if $\rho_{\delta_{error}}$ is improved, *i.e.* with a best *a posteriori* identification of the nominal model G_o, as explained in section 7.2.1.

Next, ρ_o is computed which indicates the expected controller order. Here, the model plus the performance and robustness weight orders, 4 and 2 respectively, produce coherent values of ρ_o with the resulting controller orders. The best values of ρ_o produce the following S/A selection set $\mathcal{S}_{\rho_o} = \{3\}$, which coincides with the lowest controller order 57, obtained *a posteriori* from the design. For reasons that will come clear at the end of the example, this selection needs to be expanded to higher values of ρ_o, so that new S/A pairs will allow a valid intersection with other

i pair	Actuator	Sensor	Attenuation	K order	ρ_o	ρ_{p_d}	$\rho_{\delta_{error}}$	ρ_m
1	279cm	415cm	**8.4dB**	76	0.0141	1	0.9937	**0.742**
2	279cm	295cm	**8.3dB**	66	0.0164	**1**	**0.9987**	0.5469
3	293cm	415cm	6.4dB	**57**	**0.019**	1	0.9953	0.6636
4	293cm	295cm	7.6dB	70	0.0154	1	0.9979	0.5453
5	307cm	415cm	8.1dB	62	0.0175	1	0.9980	0.5462
6	307cm	295cm	6.2dB	64	0.0169	1	0.9954	0.3928
7	322cm	415cm	7.9dB	72	0.0149	1	0.9961	0.5461
8	322cm	295cm	0.9dB	64	0.0169	0	0.9753	0.5573

Table 7.2: S/A set measures, the best ones in boldface

sets, therefore $\mathcal{S}_{\rho_o} = \{3, 5, 6, 8, 2\}$.

In addition, the performance measure ρ_{p_d} is computed which is illustrated in Table 7.2, and filters out one S/A pair obtaining the selection $\mathcal{S}_{\rho_{p_d}} = \{1, 2, 3, 4, 5, 6, 7\}$[4].

Finally, other measures are computed in order to produce their respective selection sets, see Table 7.3. In cases where these measures are very close to each other for all S/A pairs, there is no relevant information that can be produced, *i.e.* no useful filtering criteria. This is indeed what happens with values of ρ_Ω which are equal to one at all S/A locations, meaning that $\Omega_p = \Omega$. A similar result holds for $\rho_{\delta_{error}}$, *i.e.* $\max_{\omega \in \Omega} e_{rel}(\jmath\omega) \simeq 0$, which means that all identifications have been made correctly. After discarding ρ_Ω and $\rho_{\delta_{error}}$ as non-deciding measures, all other performance measures have been considered (see Tables 7.2 and 7.3), and their respective selection sets have been calculated:

$$\mathcal{S}_{\rho_m} = \{1, 3, \mathbf{2}\} \tag{7.33}$$

$$\mathcal{S}_{\rho_{\gamma_{\min}}} = \{6, 4, \mathbf{2}\} \tag{7.34}$$

As mentioned previously, the set of best locations obtained from performance and implementation measures do not intersect in general, due to the fact that they treat different issues. This case is no exception, and for that reason set $\mathcal{S}_{\rho_o} = \{3, 5, 6, 8, 2\}$ has been expanded. As a

---

[4]Note from Figure 7.2 that some pairs don't satisfy the robust performance bound in (7.18), which is not critical from the selection point of view, if at least the pair containing $\overline{\gamma}_{\min}$ does meet (7.18) and thus robust performance can be guaranteed *a priori* for this pair. This is because $2\overline{\gamma}$ is an upper bound on γ_{RP}, see (7.32). Hence, discarding pairs using $2\overline{\gamma}$ instead of using γ_{RP} just adds more conservativeness to the selection. A less conservative filtering could be achieved using γ_{RP}, but this can only be performed *a posteriori* of the controller design (7.30).

i **pair**	$\rho_{\gamma_{\min}}$
1	0.3182
2	0.921
3	0.625
4	0.9859
5	0.5512
6	**1**
7	0.4467
8	0.073

Table 7.3: S/A *a posteriori* measures

conclusion, the optimal S/A location in this case can be computed as follows:

$$\mathcal{S}_{opt} \;=\; \mathcal{S}_{\rho_{p_d}} \cap \mathcal{S}_{\rho_m} \cap \mathcal{S}_{\rho_{\gamma_{\min}}} \cap \mathcal{S}_{\rho_o} = \{2\} \tag{7.35}$$

This pair is also one of the best positions suggested by the controller performance implemented *a posteriori* , together with $i = 1$ as presented in Table 7.2. Therefore it experimentally validates the measures and the methodology. In Figure 7.2 the bounds for γ_i are posed, as well as for γ_{z_i} and weighted attenuation (λ_i) for each pair. Note that, as shown in (7.32), λ_i is bounded by $\underline{\gamma}_i$ and $2\overline{\gamma}_i$ which also validates the results. It can also be noted that the dash-dot S/A pair (*i.e.* $i = 8$) is filtered using the criteria given by ρ_{p_d}.

To be consistent with the theory, full order $\mathcal{H}_\infty$ controllers were implemented in real time using the hardware in our laboratory. Nevertheless from a practical viewpoint, a further controller order reduction using Hankel values (see section 7.1) may be used, taking care of not significantly decreasing the performance obtained previously.

Finally, an *a posteriori* reconsideration of the best S/A pair is made, as commented in definition 7.5 and section 7.2.1. In this case, the lowest ρ_m and the highest $\rho_{\gamma_{\min}}$ apply to case $i = 6$. This indicates that it may potentially produce a better performance than pair $i = 2$, with the adequate changes in W_δ. In fact, a better fit between W_δ and e_{rel} produced new values for $i = 6$: $\rho_m = 0.68$ and $\overline{\gamma} = 0.4$, which consequently produced a new set of measures:

$$\mathcal{S}_{\rho_m} = \{1, \mathbf{6}, 3\} \tag{7.36}$$

$$\mathcal{S}_{\rho_{\gamma_{\min}}} = \{\mathbf{6}, 4, 2\} \tag{7.37}$$
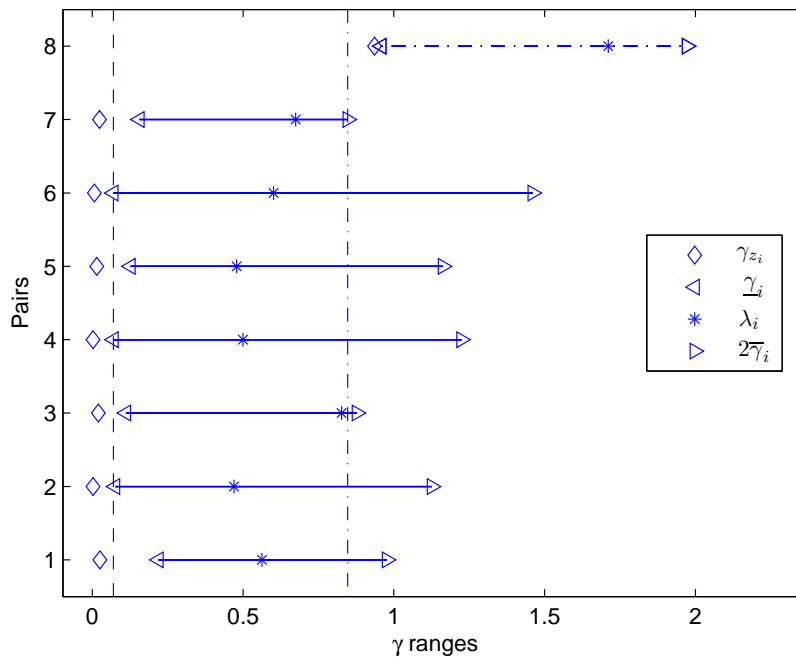
Figure 7.2: γ ranges for all sets.

whose intersection results in $\mathcal{S}_{opt} = \{6\}$. After controller implementation at this S/A location, $\lambda = 0.334$ has been computed and an attenuation of 11.8 dB has been obtained. Note that (7.32) still holds, which also validates the results. Therefore, pair $i = 6$ has become now the best position suggested by the controller performance, which experimentally validates the measures and the methodology again.

After applying the selection methodology presented here, robust performance condition (7.30) must be checked *a posteriori* of the robust controller design, if the bound in (7.18) is not fulfilled for the pair selected.

7.4 Future Research Issues

Future work needs to be made to improve this measure, considering less conservative measures for robust performance in controller free conditions, as well as exploring polynomial time

computation using the ideas of checking subsets (supersets) of nonviable (viable) S/A sets, as indicated in [vdWdJ01]. The weight determination which combines all measures into a single one could be very useful, but practical rules to determine the corresponding weights should be studied. Validation of the measures against experimental model of a 3D cavity, located in the same laboratory as the duct in Figure 3.1, would be also an interesting result.

CHAPTER 8

CONCLUDING REMARKS

In this work, a parametric/dynamic (control oriented) robust identification technique applied to ANC in a duct has been considered. This identification procedure is well-suited for this application according to physical modeling, since each mode in the duct has a clear frequency peak which can be fitted by a second order model. This reduces drastically the model order and, in turn, the controller order. In addition, the outcome of the identification, a family of models with dynamic bounded uncertainty, fits exactly the $\mathcal{H}_\infty$ robust controller design method. Also, the main compromises, driven by practical issues, that limit the achievable performance have been discussed. Limitations imposed by nonminimum phase zeros and controller model order have been pointed out, and explicitly related to performance and robustness. Theoretical and experimental results were compared, and the overall experimental attenuation is very good, as compared with other works in the area. General hybrid (FF/FB) control structures have been also implemented and compared with feedback and feedforward loops separately.

Finally, the S/A allocation has been also considered as part of the whole ANC problem. Several measures of S/A location have been defined focused on closed loop performance, robustness and controller order. These can be computed before building and testing the controller, which minimizes the combinatorial search to seek the best S/A location. These measures produce sets which are finally intersected in order to narrow down the search for the best S/A location. An experimental example based on active noise control in a tube is used to validate the measures and the methodology.

8.1   Contributions

In the context described in the last paragraphs, the main general contributions provided by this work are enumerated next:

- To apply a robust (control oriented) identification to an ANC system, with a deterministic worst-case criteria in order to design a robust controller. In particular, based on the experimental knowledge of low frequency modes, a parametric/dynamic model identification method [PSS99, BMS01] has been applied. This produces a multiplicative global uncertain set to describe the physical plant, which exactly fits the robust controller design framework.

- To present a deep analysis of the compromises and practical issues which arise in the robust identification and controller design stages for an ANC system. These are mainly derived from the compromises between identification and control, performance and robustness, feedback limitations, model and controller order, and implementation issues.

- To implement the robustly normalized σ-modification algorithm in a FF and an hybrid (FF/FB) ANC fashion, and compare all the resulting structures with relevant practical performance results.

- To develop a novel and general (*i.e.* applicable to many practical applications) optimal S/A allocation measure previous to controller design and implementation, combining relevant issues concerning performance, robustness and implementation, and test it against ANC system.

8.2   Directions for Future Research

Finally, some issues that could be taken into account by interested researchers in this area are pointed out next:

- A procedure to decide beforehand whether to use linear or nonlinear hybrid controllers, based on the desired performance, could be helpful. In some sense this would generalize the method followed in this work, in the case of hybrid *versus* FF controllers.

- To test and compare another robust FF algorithms in an ANC application, *e.g.* the ones presented in [IS96].

In order to improve the S/A allocation measure, future work could follow next directives:

- To consider less conservative measures for robust performance in controller free conditions.

- To explore polynomial time computation using the ideas of checking subsets (supersets) of nonviable (viable) S/A sets, as suggested in [vdWdJ01].

- Weight determination to combine all measures presented in Chapter 7 into a single one could be very useful, but practical rules to determine the corresponding weights should be studied.

- To validate the measures stated in Chapter 7 against experimental model of a 3D cavity (located in the same laboratory as the model of the duct used throughout the work (Figure 3.1) would be also an interesting result.

APPENDIX A

ROBUST FEEDBACK CONTROLLER SYNTHESIS ALGORITHM

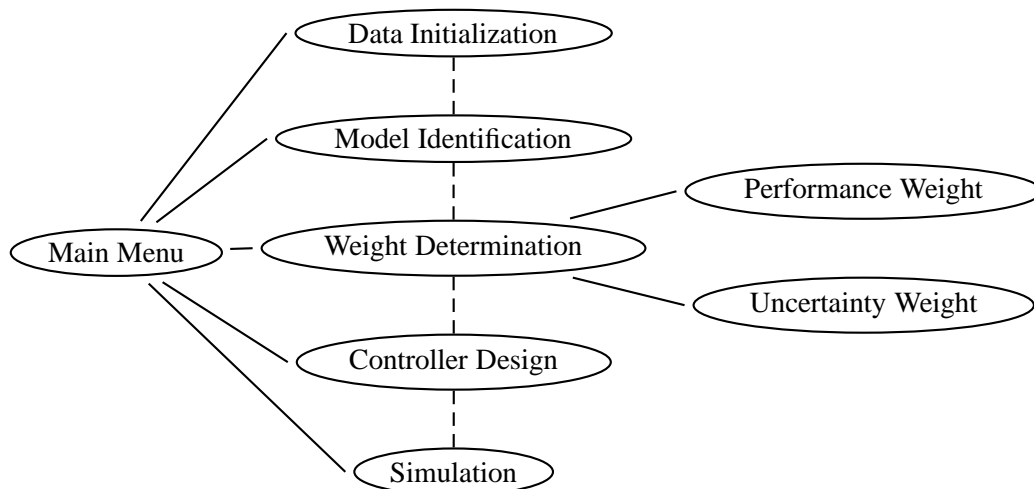The main structure of the program is as follows:

Figure A.1: Controller design algorithm main diagram

Deeply analyzing each step of the algorithm's diagram in Figure A.1, the detailed pseudo-code in Algorithm A.1 may be defined:

Algorithm A.1 Robust Controller design algorithm

1: Introduce Main Menu flag

   $[DataInitialization; ModelIdentification; WeightIntroduction; ControllerDesign; Simulation]$

2: **if** Data Initialization **then**

3:     Introduce experimental data

4:     Select data bandwidth Ω

5:     Choose parametric identification frequency points ω_p

6:     Choose non-parametric identification frequency points ω_{np}

7: **end if**

8: **if** Model Identification **then**

9:     Adjust Kautz basis

10:     **while** Model not accepted **do**

11:         Model order reduction

12:         Accept/reject model identified by comparison against experimental data

13:     **end while**

14: **end if**

15: **if** Weight Introduction **then**

16:     **if** Performance Weight W_p **then**

17:         Introduce W_p coefficients

18:         Compare against exogenous variable (w) spectra

19:         Accept/Reject W_p

20:     **end if**

21:     **if** Uncertainty Weight W_δ **then**

22:         Introduce W_δ coefficients

23:         Compare against relative error (e_{rel}) spectra

24:         Accept/Reject W_δ

25:     **end if**

26: **end if**

27: **if** Controller Design **then**

28:     Introduce γ bounds and iteration tolerance of $\mathcal{H}_\infty$ problem solver algorithm

29:     **if** Feasible loop **then**

30:         Controller order reduction

31:         **if** Robust Performance achieved **then**

32:             *Robust Controller K is obtained*

33:             Obtain SOS controller model for final implementation

34:         **end if**

35:     **end if**

36: **end if**

37: **if** Simulation **then**

38:     Check Robust Controller K designed on Step 32 against Simulink's duct model

39: **end if**

Some extra investments implemented to this code are pointed out next:

- Data introduction front-end for G_o identification

- Generalization to different input data fundamental frequency, bandwidth and sample rate

- Arrangement for compatibility with DSpace software data types

- Model error measure in Ω_p to decide wether reject G_o obtained or not

- Interface to recover data used in previous runs (*e.g.* weights, γ bounds)

- Poles scaling of K for fragile loops

- Use of γ bounds and iteration tolerance in the Riccati $\mathcal{H}_\infty$ solver in order to avoid certain numerical problems

- Implementation of K using SOS structure in order to prevent numerical perturbations of pole locations in high order models

- Design of NP controllers for S/A measure computation

BIBLIOGRAPHY

[And85] Brian D. O. Anderson. Adaptive systems, lack of persistency of excitation and bursting phenomena. *Automatica*, 21(3):247 – 258, 1985.

[BCPS05] Gary Balas, Richard Chiang, Andy Packard, and Michael Safonov. *Robust Control Toolbox*. The Mathworks, Inc., 2005.

[BEN91] C.C. Boucher, S.J. Elliott, and P.A. Nelson. Effect of errors in the plant model on the performance of algorithms for adaptive feedforward control. *Radar and Signal Processing, IEE Proceedings F*, 138(4):313–319, 1991.

[BGR90] J. Ball, I. Gohberg, and L. Rodman. *Interpolation of Rational Matrix Functions,Operator Theory: Advances and Applications*, volume 45. Birkhäuser, 1990.

[BK08] Christian Benatzky and Martin Kozek. Influence of actuator size and location on robust stability of actively controlled flexible beams. In *Proceedings of IFAC, Seoul*, 2008.

[BL97] M.R. Bai and H. Lin. Comparison of Active Noise Control Structures in the Presence of Acoustical Feedback by using the $\mathcal{H}_\infty$ Synthesis Technique. *Journal of Sound and Vibration*, 206(4):453–471, 1997.

[BL98] M.R. Bai and H. Lin. Plant uncertainty analysis in a duct active noise control problem by using the $\mathcal{H}_\infty$ theory. *Journal of Acoustical Society of America*, 104(1):237–247, July 1998.

[BMS01] Darío Baldelli, M. Cecilia Mazzaro, and Ricardo S. Sánchez Peña. Robust identification of lightly damped flexible structures by means of orthonormal bases. *IEEE Transactions on Control Systems Technology*, 9(5):696–707, 2001.

[CA00] Jean Claude Carmona and Victor Alvarado. ANC of a Duct using Robust Control Theory. *IEEE Transactions on Control Systems Technology*, 8(6):930–8, 2000.

[CDL86] C.C. Chu, J. Doyle, and E.B. Lee. The general distance problem in $\mathcal{H}_\infty$ optimal control theory. *International Journal of Control*, 44(2):565–596, 1986.

[CG00] Jie Chen and Guoxiang Gu. *Control-Oriented System Identification - An $\mathcal{H}_\infty$ Approach*. Willey Inter-Science, 2000.

[CMS07] Miquel À. Cugueró, Bernardo Morcego, and Ricardo S. Sánchez-Peña. *Identification and Control: The Gap between Theory and Practice*, chapter 8. Identification and Control Structure Design in Active (Acoustic) Noise Control, pages 203–44. Springer-Verlag, 2007.

[CSM+05] M.À. Cugueró, R. S. Sánchez Peña, A. Masip, J. Quevedo, and V. Puig. Comparación de algoritmos feedforward adaptativos para el control activo de ruido en un conducto. In *TecniAcústica 2005*, Terrassa, Barcelona, 2005.

[CSPn09] M.À. Cugueró and R. Sánchez Peña. Control-oriented Sensor/Actuator Location Measures. *Control Engineering Practice*, (submitted), 2009.

[DF99] M.A. Demetriou and F. Fahroo. Optimal location of actuators for control of a 2-D structural acoustic model. In *Conference on Decision and Control*, pages 4290–4295, Phoenix, USA, December 1999.

[DFSVB01] P. De Fonseca, P. Sas, and H. Van Brussel. Robust design and robust stability analysis of active noise control systems. *Journal of Sound and Vibration*, 243(1):23–42, May 2001.

[DFT92] John C. Doyle, B. Francis, and A. Tannembaum. *Feedback Control Theory*. Maxwell/Macmillan, 1992.

[DGKF89] John C. Doyle, Keith Glover, Pramod P. Khargonekar, and Bruce A. Francis. State-space solutions to standard $\mathcal{H}_2$ and $\mathcal{H}_\infty$ control problems. *IEEE Transactions on Automatic Control*, 34(8):831–847, August 1989.

[DH09] Pooya Davari and Hamid Hassanpour. Designing a new robust on-line secondary path modeling technique for feedforward active noise control systems. *Signal Processing*, 89(6):1195–1204, June 2009.

[Doy84] J. Doyle. *ONR/Honeywell Workshop on Advances in Multivariable Control*. (Lecture Notes), 1984.

[FBL93] P.L. Feintuch, N.J. Bershad, and A.K. Lo. A frequency domain model for 'filtered' LMS algorithms-stability analysis, design, and elimination of the training mode. *Signal Processing, IEEE Transactions on*, 41(4):1518–1531, 1993.

[FHMT03] J.S. Freudenberg, C.V. Hollot, R.H. Middleton, and V. Toochinda. Fundamental Design Limitations of the General Control Configuration. *IEEE Transactions on Automatic Control*, 48(8):1355–70, 2003.

[FL85] J.S. Freudenberg and D.P. Looze. Right half plane poles and zeros and design tradeoffs in feedback systems. *IEEE Transactions on Automatic Control*, 30(6):555–565, 1985.

[Gaw97] W. Gawronski. Actuator and Sensor Placement for Structural Testing and Control. *Journal of Sound and Vibration*, 208(1):101–109, 1997.

[Gaw99] W. Gawronski. Letters to the Editor: Simultaneous Placement of Actuators and Sensors. *Journal of Sound and Vibration*, 228(4):915–922, 1999.

[Gaw04] W.K. Gawronski. *Advanced Structural Dynamics and Active Control of Structures*. Springer-Verlag New York, Inc., 2004.

[GLD$^+$91] K. Glover, D. J. N. Limebeer, J. C. Doyle, E. M. Kasenally, and M. G. Safonov. A characterization of all solutions to the four block general distance problem. *SIAM Journal on Control and Optimization*, 29(2):283–324, 1991.

[Glo84] K. Glover. All optimal Hankel norm approximations of linear multivariable systems and their L^∞-error bounds. *International Journal of Control*, 39(6):1115–1193, July 1984.

[GS84] G. Goodwin and K. Sin. *Adaptive Filtering, Prediction and Control*. Prentice Hall, New Jersey, 1984.

[GSPnM07] R. García, R. Sánchez Peña, and J. Mancilla. Real time stable identification: A Nehari/SOS approach. In *Proceedings of European Control Conference*, Kos, Greece, 2007.

[Han04] Colin H. Hansen. Current and Future Industrial Applications of Active noise Control. In *ACTIVE 04*, pages 1–18, 2004. (Plenary talk).

[HAV$^+$96] J. Hong, J.C. Akers, R. Venugopal, M.N. Lee, A.G. Sparks, P.D. Washabaugh, and D.S. Bernstein. Modeling, identification and feedback control noise in an acoustic duct. *IEEE Transactions on Control Systems Technology*, 4(3):283–291, 1996.

[HB98] J. Hong and Dennis Bernstein. Bode integral constraints, colocation, and spillover in active noise and vibration control. *IEEE Transactions on Control Systems Technology*, 6(1):111–120, 1998.

[HJN91] J. Helmicki, C. Jacobson, and C. Nett. Control Oriented System Identification: A worst case/deterministic approach in $\mathcal{H}_\infty$. *IEEE Transactions on Automatic Control*, 36(10):1163–1176, 1991.

[IS96] P. Ioannou and J. Sun. *Robust Adaptive Control*, chapter 8. Robust Adaptive Laws, pages 530–633. Prentice Hall, Inc, 1996.

[JT98] B. De Jager and O. Toker. Complexity of input output selection. In A. Beghi, L. Finesso, and G. Picci, editors, *International Symposium on Mathematical Theory of Networks and Systems*, pages 597–600, Polygrafo, Padova, 1998.

[KBG92] P.J. Kootsookos, R.R. Bitmead, and M. Green. The Nehari shuffle: FIR(q) filter design with guaranteed error bounds. *Signal Processing, IEEE Transactions on*, 40(8):1876–1883, 1992.

[KD70] R.E. Kalman and N. DeClaris, editors. *Aspects of Network and Systems Theory*, chapter Adaptive Filters, pages 563–587. Rinehart and Winston, 1970.

[KF03] Y. Kobayashi and H. Fujioka. Active noise control of one-dimensional duct via sampled-data $\mathcal{H}_\infty$ control. In *Conference on Decision and Control*, pages 3900–3904, Las Vegas, December 2003.

[KM95] S.M. Kuo and D.R. Morgan. *Active Noise Control Systems: Algorithms and DSP Implementations*. John Wiley and Sons, New York, 1995.

[KPM03] O.E. Kaiser, S.J. Pietrzko, and M. Morari. Feedback control of sound transmission through a double glazed window. *Journal of Sound and Vibration*, 263(4):775–795, 2003.

[KTMX95] S. K. Katsikas, D. Tsahalis, D. Manolas, and S. Xanthakis. A genetic algorithm for active noise control actuator positioning. *Mechanical Systems and Signal Processing*, 9(6):697–705, 1995.

[LAKB01] S. Leleu, H. Abou-Kandil, and Y. Bonnassieux. Piezoelectric Actuators and Sensors Location for Active Control of Flexible Structures. *IEEE Transactions on Instrumentation and Measurement*, 50(6):1577–1582, 2001.

[LBMP94] J.H. Lee, R.D. Braatz, M. Morari, and A. Packard. Screening tools for robust control structure selection. *Automatica*, 31(2):229–235, 1994.

[LKJS88] D.J.N. Limebeer, E.M. Kasenally, I. Jaimoukha, and M.G. Safonov. All solutions to the four block general distance problem. In *Decision and Control, 1988., Proceedings of the 27th IEEE Conference on*, pages 875–880 vol.1, 1988.

[Lue34] P. Lueg. *Process of silencing sound oscillations*. U.S. Patent 043,416, 1934.

[MC01] B. Morcego and M.À. Cugueró. Comparación de implementaciones en C y Matlab de filtros adaptativos para DSP. In *Proceedings of XXII Jornadas de Automática*, Bellaterra, Barcelona, 2001.

[Moo81] B.C. Moore. Principal component analysis in Linear systems: Controllability, Observability and Model reduction. *IEEE Transactions on Automatic Control*, 26(1):17– 32, 1981.

[Mor80] D. Morgan. An analysis of multiple correlation cancellation loops with a filter in the auxiliary path. *Acoustics, Speech and Signal Processing, IEEE Transactions on*, 28(4):454–467, 1980.

[Mor08] K. Morris. LQ-optimal actuator location and norm convergence of Riccati operators. In *Decision and Control, 2008. CDC 2008. 47th IEEE Conference on*, pages 209–214, 2008.

[MPG95] P.M. Mäkilä, J.R. Partington, and T.K. Gustafsson. Worst-case Control-relevant Identification. *Automatica*, 31(12):1799 –1819, 1995.

[MPS04] M. C. Mazzaro, P. A. Parrilo, and R. S. Sánchez Peña. Robust Identification Toolbox. *Latin American Applied Research*, 34(2):91–100, 2004.

[MS80] M. Morari and G. Stephanopoulos. Studies in the synthesis of control structures for chemical processes: Part II: Structural aspects and the synthesis of alternative feasible control schemes. *A.I.Ch.E. Journal*, 26(2):232–246, 1980.

[MS04] M.C. Mazzaro and M. Sznaier. Convex necessary and sufficient conditions for frequency domain model (in)validation under SLTV structured uncertainty. *Automatic Control, IEEE Transactions on*, 49(10):1683–1692, 2004.

[Nar86] K.S. Narendra. *Adaptive and Learning Systems: Theory and Applications*. Plenum Press, New York, 1986.

[NE92] P.A. Nelson and S.J. Elliot. *Active Control of Sound*. Academic Press, 1992.

[OM53] H.F. Olson and E.G. May. Electronic sound absorber. *Journal of Acoustical Society of America*, 25:1130–1136, 1953.

[OM94] P. Van Overschee and B. De Moor. N4SID: subspace algorithms for the identification of combined deterministic and stochastic systems. *Automatica*, 30(1):75–93, 1994.

[OT89] Romeo Ortega and Yu Tang. Robustness of adaptive controllers–A survey. *Automatica*, 25(5):651 – 677, 1989.

[OWPB00] R.T. O'Brien Jr, J.M. Watkins, G.E. Pipert, and D.C. Baumannt. $\mathcal{H}_\infty$ Active Noise Control of Fan Noise In An Acoustic Duct. In *Proceedings of American Control Conference*, pages 3028–3032, Chicago, June 2000.

[Par78] S. Parrot. On a quotient norm and the Sz–Nagy Foais lifting theorem. *Journal of Functional Analysis*, 30:311–328, 1978.

[PnCM+08] R. S. Sánchez Peña, M. À. Cugueró, A. Masip, J. Quevedo, and V. Puig. Robust identification and feedback design: An active noise control case study. *Control Engineering Practice*, 16(11):1265–1274, Nov 2008.

[PP06] Suwit Pulthasthan and Hemanshu Pota. Optimal actuator–sensor Placement for Acoustic Cavity. In *Conference on Decision and Control*, pages 1984–1989, San Diego, USA, 2006.

[PP08] Suwit Pulthasthan and Hemanshu R. Pota. The optimal placement of actuator and sensor for active noise control of sound-structure interaction systems. *Smart Materials and Structures*, 17:1–11, 2008.

[PSS99] P. A. Parrilo, R. S. Sánchez Peña, and M. Sznaier. A parametric extension of mixed time/frequency robust identification. *IEEE Transactions on Automatic Control*, 44(2):364–369, 1999.

[PSSI98] Pablo A. Parrilo, Mario Sznaier, Ricardo S. Sánchez Peña, and Tamer Inanc. Mixed time/frequency-domain based robust identification. *Automatica*, 34(11):1375–1389, 1998.

[Rao93] B.D. Rao. Adaptive IIR filtering using cascade structures. In *Signals, Systems and Computers, 1993. 1993 Conference Record of The Twenty-Seventh Asilomar Conference on*, pages 194–198 vol.1, 1993.

[RE99] B. Rafaely and S.J. Elliot. $\mathcal{H}_2/\mathcal{H}_\infty$ active control of sound in a headrest: Design and implementation. *IEEE Transactions on Control Systems Technology*, 7(1):79–84, 1999.

[RF95] C. E. Ruckman and C. R. Fuller. Optimizing actuator locations in active noise control systems using subset selection. *Journal of Sound and Vibration*, 186(3):395–406, 1995.

[RGL02] W. Reinelt, A. Garulli, and L. Ljung. Comparing different approaches to model error modelingin robust identication. *Automatica*, 38:787–803, 2002.

[RN08] K. Ramesh and S. Narayanan. Active vibration control of beams with optimal placement of piezoelectric sensor/actuator pairs. *Smart Materials and Structures*, 17:1–15, 2008.

[Rom99] J. Romeu. *Atenuación de Ruido Industrial de Baja Frecuencia Mediante la Técnica de Control Activo de Ruido*. PhD thesis, ETSEIAT, Universitat Politècnica de Catalunya, 1999.

[SBG97] M.M. Serón, J.H. Braslavsky, and G.C. Goodwin. *Fundamental Limitations in Filtering and Control*. Springer, 1997.

[SBS+09] C. Spier, J. C. Bruch, Jr., J. M. Sloss, S. Adali, and I. S. Sadek. Placement of Multiple Piezo Patch Sensors and Actuators for a Cantilever Beam to Maximize Frequencies and Frequency Gaps. *Journal of Vibration and Control*, 15(5):643–670, May 2009.

[SCM+05] R. S. Sánchez Peña, M.À. Cugueró, A. Masip, J. Quevedo, and V. Puig. Acoustic noise suppression: Compromises in identification and control. In *2nd. International Conference on Informatics in Control, Automation and Robotics*, Barcelona, Spain, 2005.

[SFN08] H. Salmasi, R. Fotouhi, and P. N. Nikiforuk. Vibration control of a flexible link manipulator using smart structures. In *Proceedings of IFAC*, Seoul, South Korea, 2008.

[SH94] S.D. Snyder and C.H. Hansen. The effect of transfer function estimation errors on the filtered-x LMS algorithm. *Signal Processing, IEEE Transactions on*, 42(4):950–953, 1994.

[SM03] M. Sznaier and M.C. Mazzaro. An LMI approach to control-oriented identification and model (In) validation of LPV systems. *Automatic Control, IEEE Transactions on*, 48(9):1619–1624, 2003.

[SMD88] S. Skogestad, M. Morari, and J.C. Doyle. Robust control of ill-conditioned plants: High purity distillation. *IEEE Transactions on Automatic Control*, 33:1092–1105, 1988.

[SP96] S. Skogestad and I. Postlethwaite. *Multivariable feedback control: Analysis and design*. Chichester, UK, Wiley., 1996.

[SPCiE08] R. S. Sánchez Peña and M. À. Cugueró i Escofet. Control-oriented sensor/actuator location measures for active noise control. In *Proceedings of IFAC World Congress*, pages 8719–8724, Seoul, South Korea, 2008.

[SS98] R. S. Sánchez Peña and M. Sznaier. *Robust Systems Theory and Applications*. John Wiley & Sons, Inc., 1998.

[Tao03] G. Tao. *Adaptive Control, Design and Analysis*. John Wiley & Sons, Ltd., 2003.

[THC02] V. Toochinda, C.V. Hollot, and Y. Chait. Disturbance attenuation in a SITO feedback control system. In *American Control Conference*, 2002.

[vdWdJ01] Marc van de Wal and Bram de Jager. A review of methods for input/output selection. *Automatica*, 37:487–510, 2001.

[Ver94] M. Verhaegen. Identification of the deterministic part of MIMO state space models given in innovations form from input-output data. *Automatica*, 30(1):61–74, 1994.

[WAN95] G.A. Williamson, J.P. Ashley, and M. Nayeri. Structural issues in cascade-form adaptive IIR filters. In *Acoustics, Speech, and Signal Processing, 1995. ICASSP-95., 1995 International Conference on*, volume 2, pages 1436–1439 vol.2, 1995.

[WL05] Jian-Da Wu and Tian-Hua Lee. Application of $\mathcal{H}_\infty$ hybrid active controller for acoustic duct noise cancellation. *International Journal of Vehicle Noise and Vibration*, 1(3/4):183–193, 2005.

[WP97] E. Walter and L. Pronzato. *Identification of Parametric Models*. Masson, 1997.

[YAN02] Y. Yamamoto, B.D.O. Anderson, and M. Nagahara. Optimal FIR approximation for discrete-time IIR filters. In *Proceedings 4th. Asian Control Conference*, number 1 in FA3, pages 2008–13, Singapore, September 2002.

[ZDG96] K. Zhou, John C. Doyle, and Keith Glover. *Robust and Optimal Control*. Prentice–Hall, 1996.